1936-24

**Advanced School on Synchrotron and Free Electron Laser Sources
and their Multidisciplinary Applications**

7 - 25 April 2008

**Small angle x-ray scattering
(Applications)**

Aldo Craievich

*University de Sao Paulo
Brazil*

SAXS. Applications

Aldo F. Craievich

Institute of Physics

University of São Paulo

Brazil

(craievich@if.usp.br)

La Habana Cuba
Julio de 2007
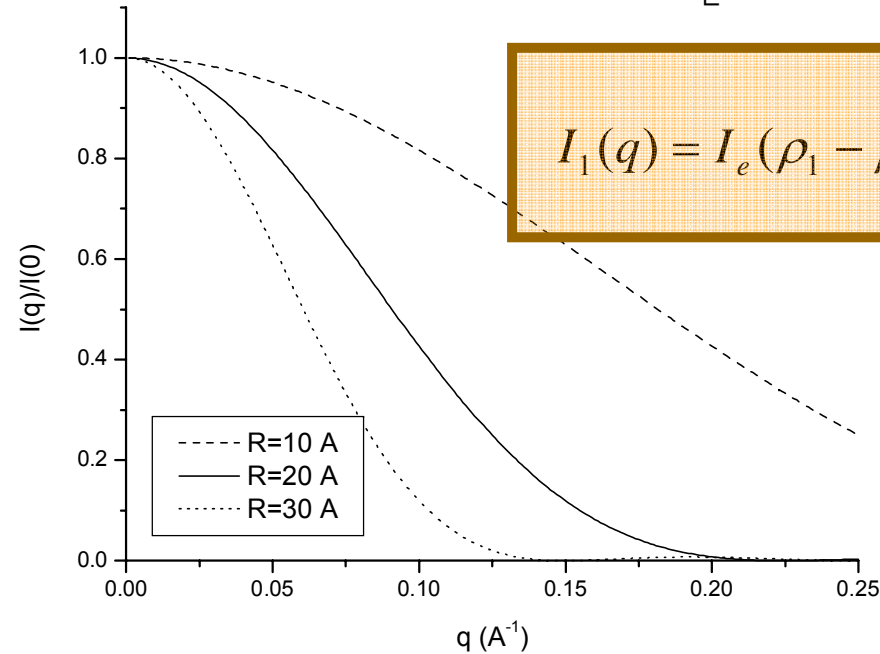
Content

SAXS - Applications

Basic reference

"Small-angle X-ray scattering by nanostructured materials". A. F. Craievich. Handbook of Sol-Gel Science and Technology, Vol II Chapter 8, Kluwer Publishers (2005)

Dilute set of spherical nano-objects embedded in a homogeneous matrix

$$I(q) = \int N(R).I_1(q,R)dR$$

$$I_1(q) = I_e(\rho_1 - \rho_2)^2 V_1 \int_0^R \left[1 - \frac{3r}{R} + \frac{1}{16}\left(\frac{r}{R}\right)^3\right] 4\pi.r^2 \frac{\sin qr}{qr} dr$$
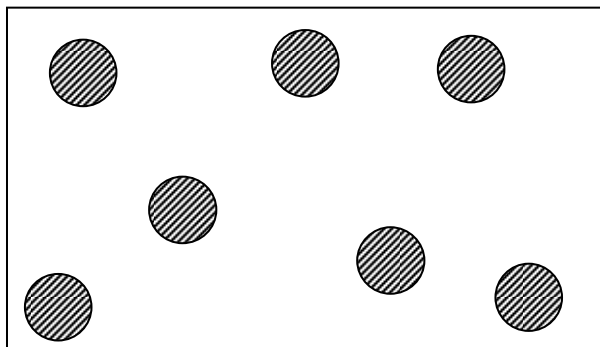
$$\gamma_0(r) = 1 - \frac{3r}{R} + \frac{1}{16}\left(\frac{r}{R}\right)^3$$

$$I_1(q) = I_e(\rho_1 - \rho_2)^2 . \left(\frac{4\pi R^3}{3}\right)^2 [\Phi(q)]^2$$
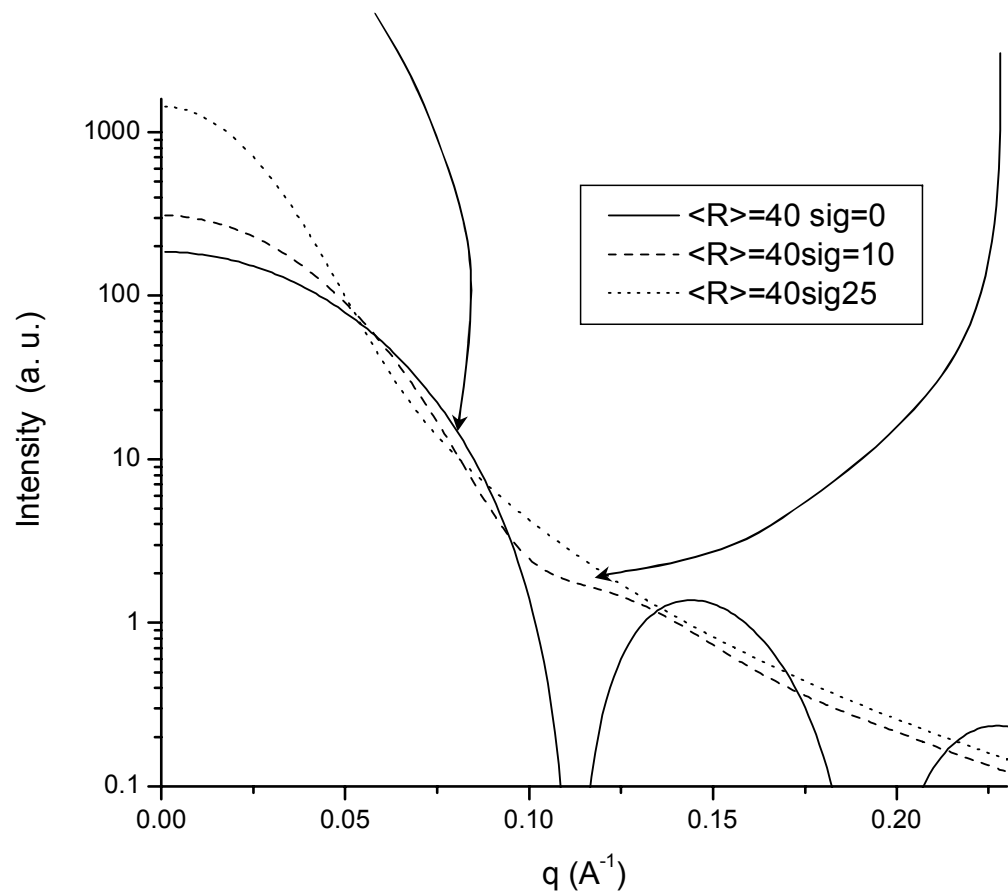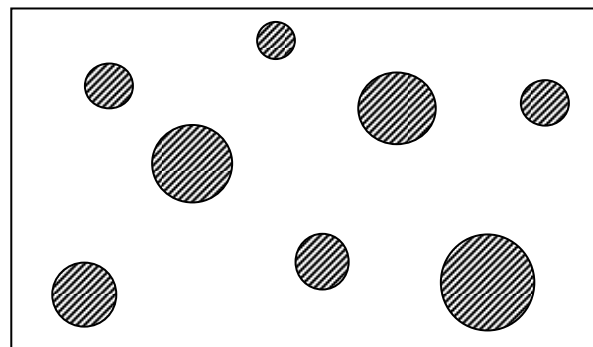

$$\Phi(q) = 3\frac{\sin qR - qR\cos qR}{(qR)^3}$$

$$I(q) = I_e(\rho_1 - \rho_2)^2 \left(\frac{4\pi}{3}\right)^2 \int N(R).R^6 \left[3\frac{\sin qR - qR\cos qR}{(qR)^3}\right]^2 dR \qquad \textbf{(1)}$$
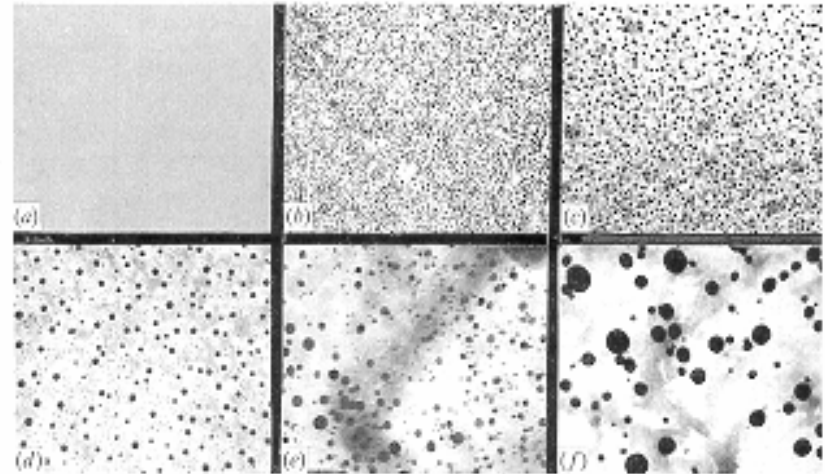
$$D(R) = \frac{4\pi}{3}R^3.N(R)$$

Identical spheres

Polydisperse set of spheres

Intensity (a. u.)

q (A^{-1})

— $\langle R \rangle$=40 sig=0
- - - $\langle R \rangle$=40sig=10
· · · $\langle R \rangle$=40sig25

Dilute set of PbTe nano-crystals embedded in a homogeneous silicate glass (Kellermann et al)

Scattering intensity curves corresponding to a dilute set of spherical PbTe nano-crystals during isothermal growth (T=650C).
The continuous line is the best fit of Eq. (1) using a Gaussian N(R) function with a time varying radius average and a constant relative standard deviation $[\sigma/\{R\}]$ =0.08. The curves were vertically displaced for clarity

$$I(q) = I_e(\rho_1 - \rho_2)^2 \left(\frac{4\pi}{3}\right)^2 \int N(R) \cdot R^6 \left[3 \frac{\sin qR - qR \cos qR}{(qR)^3}\right]^2 dR \qquad \textbf{(1)}$$
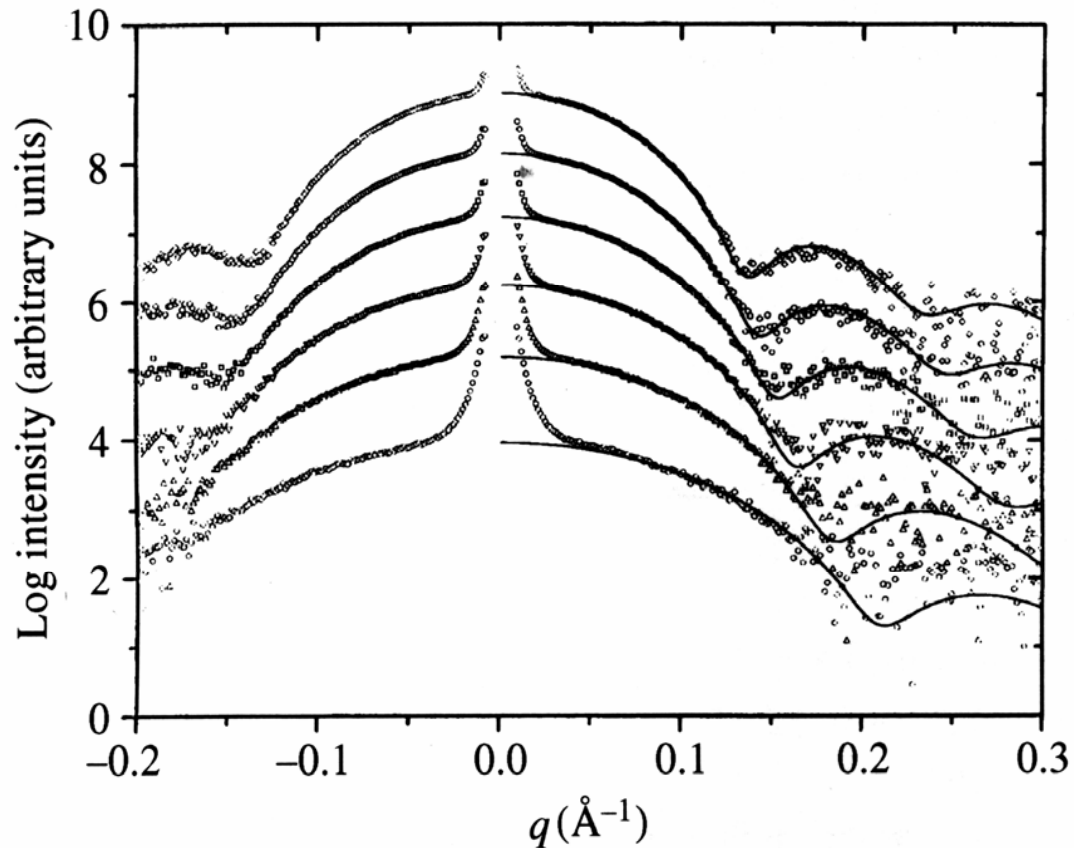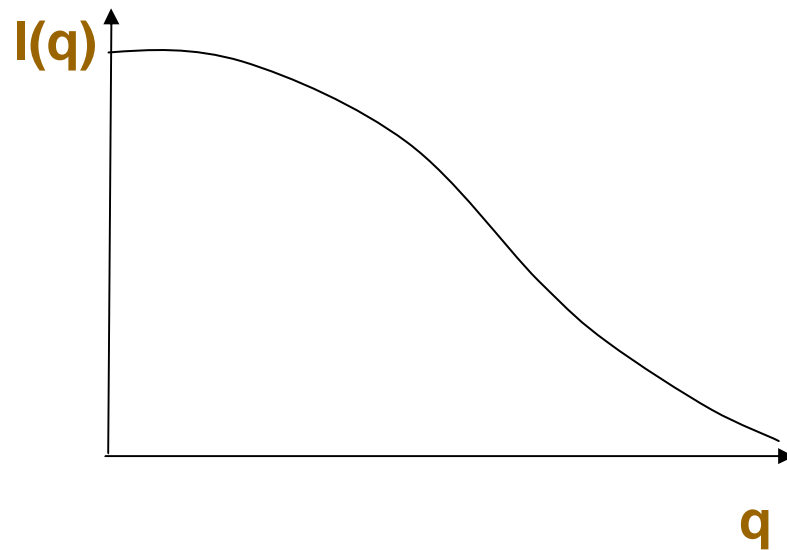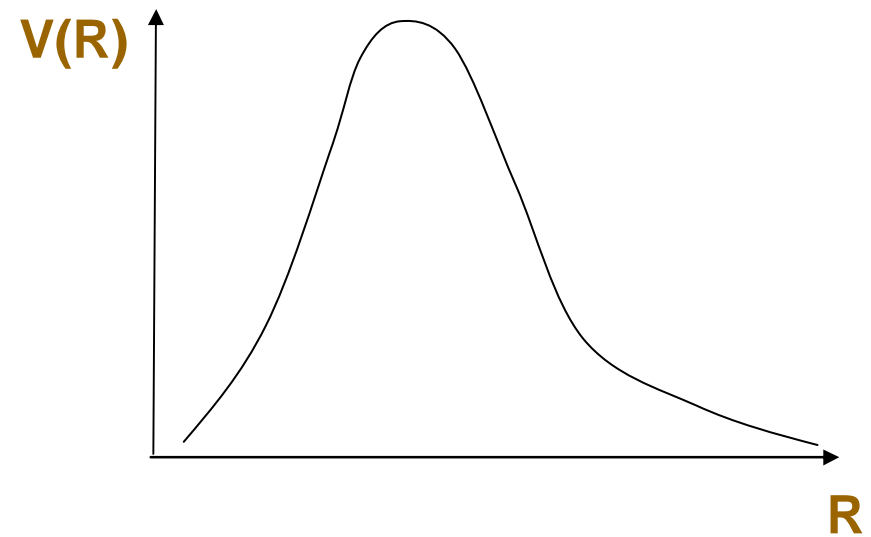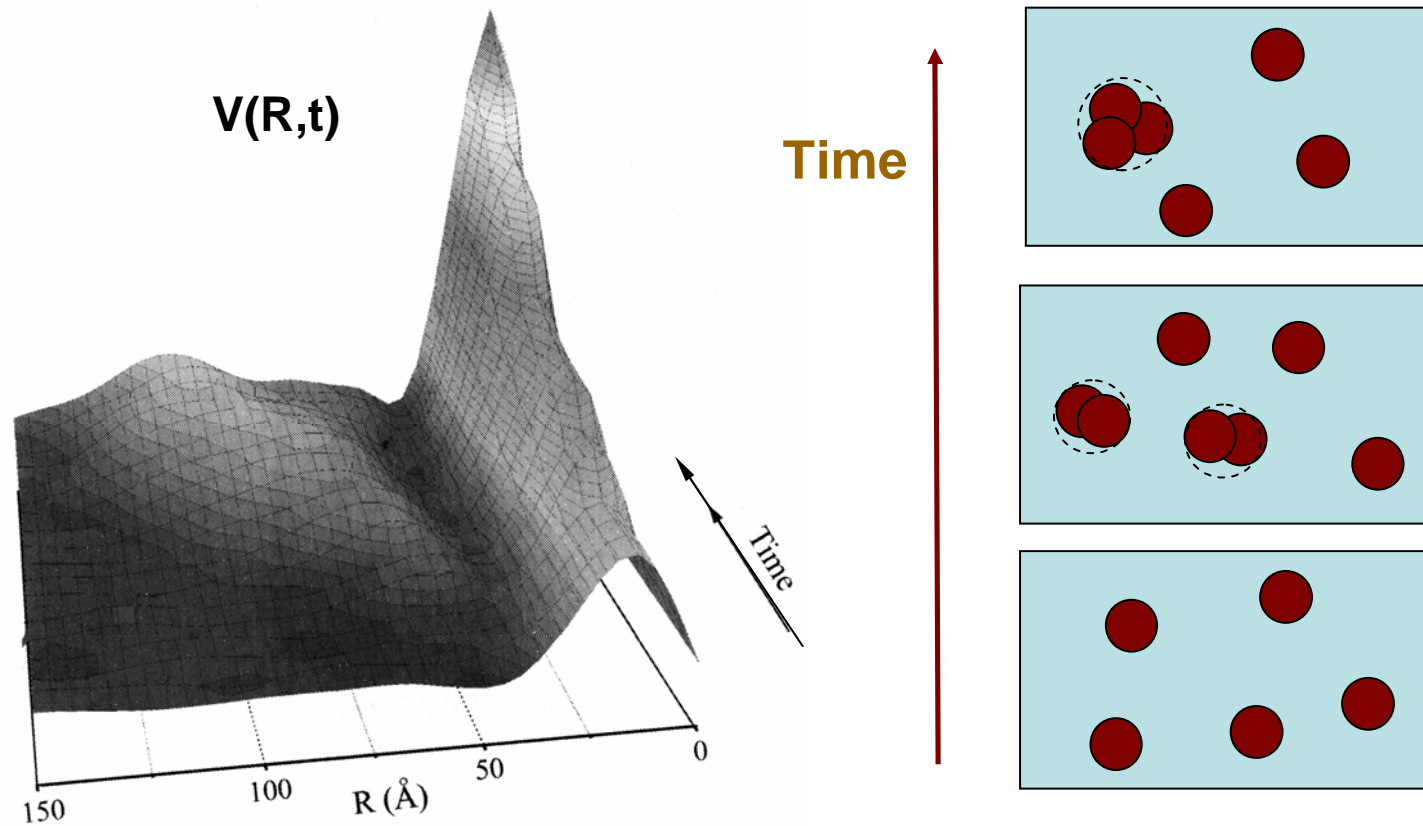
GNOM program (Svergun et al)

Input I(q)

Output V(R)=N(R)*(4/3)π.R^3

ZnO-based colloidal suspensions (Tokumoto et al).

V(R,t)

Time

Time-dependent volume distribution functions V(R,t) of ZnO colloidal particles in liquid solution.
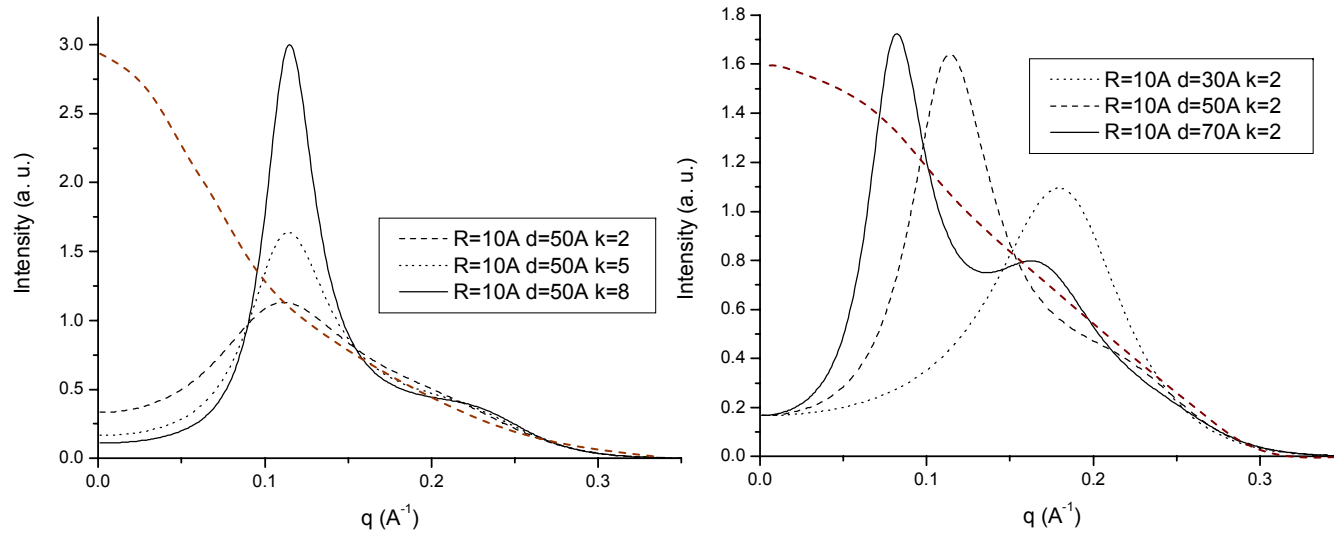Time period range:10 to 120 min.
The volume functions were derived, using the GNOM package, from jn situ SAXS measurements.

Spherical nano-objects embedded in a solid matrix
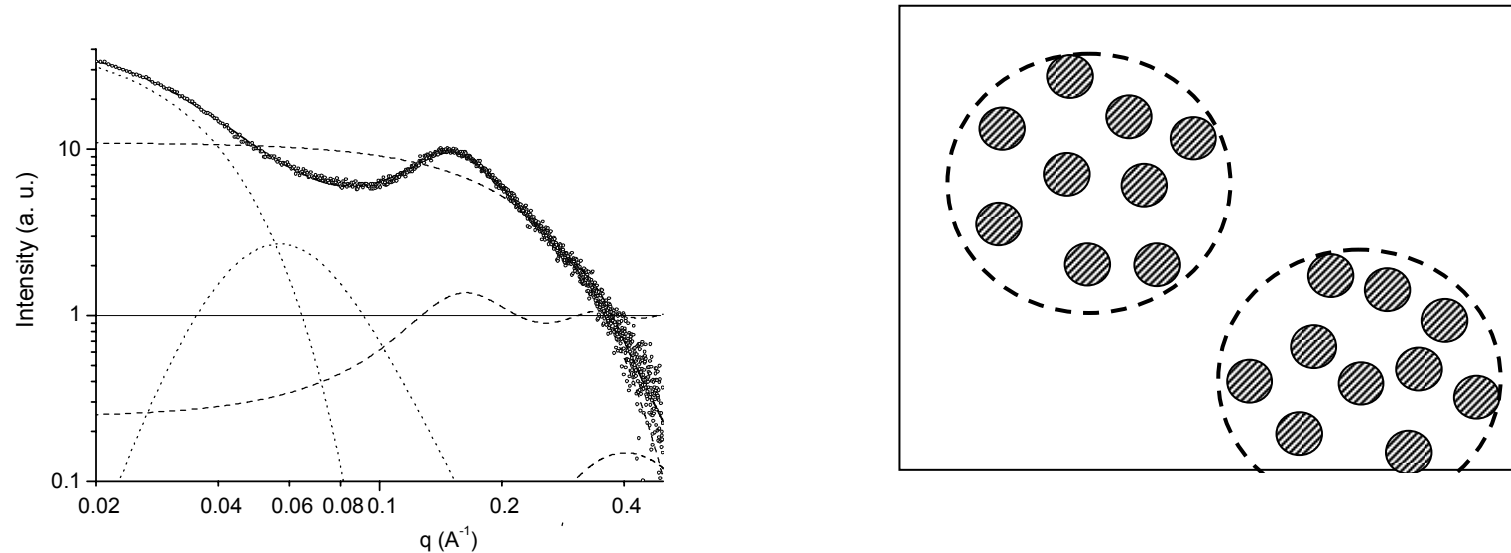## Dense systems

$$I(q) = N.I_1(q).S(q)$$

$$S(q) = \frac{1}{1 + k\Phi(qd)}$$

$$\Phi(qd) = 3\frac{\sin(qd) - qd\cos(qd)}{(qd)^3}$$

$$d = \frac{2\pi}{q_{max}}$$

Fe(II) doped di-ureasil hybrids (Silva et al)

$$I(q) = S_1(q).\left[G_1.e^{-\frac{1}{3}R_{g1}^2 q^2} + B_1.e^{-\frac{1}{3}R_c^2 q^2}\left\{\left[erf\left(qR_{g1}/6^{1/2}\right)\right]^3/q\right\}^4\right] + \left[G_2.e^{-\frac{1}{3}R_{g2}^2 q^2} + B_2.\left\{\left[erf\left(qR_{g2}/6^{1/2}\right)\right]^3/q\right\}^4\right]..(1)$$

Experimental scattering intensity from a hybrid sample
containing 0.76 weight % Fe(II).
The continuous line is the best fit of Eq. 1 to the experimental curve.
The dashed lines indicate the structure function (oscillatory curve)and theGuinier
and Porod contributions to the scattering intensity produced by siliceous clusters.
The point lines are the Guinier and Porod
contributions to the scattering intensity yielded by the coarse domains.
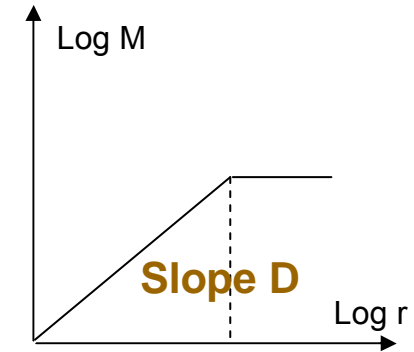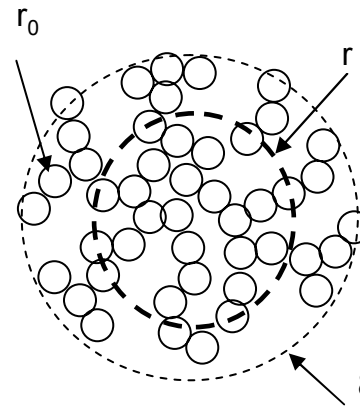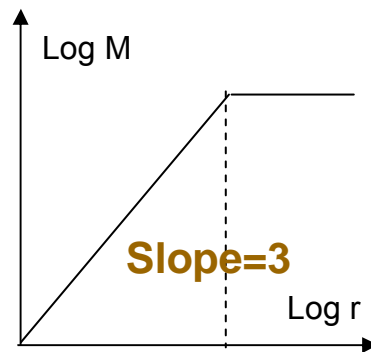
Multilevel hierarchical structure (Beaucage)

Level 1   Level 2   Log I(q)

(79)

Log q
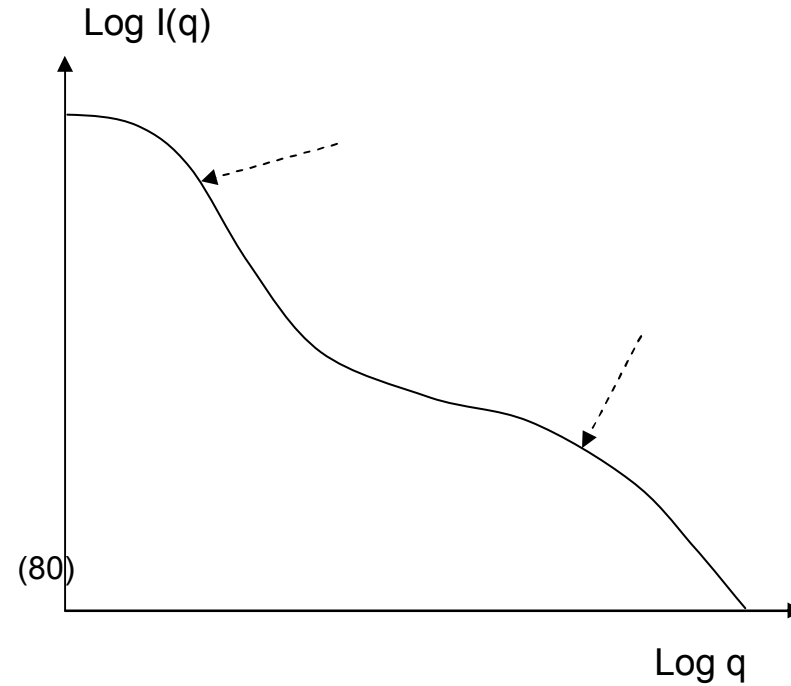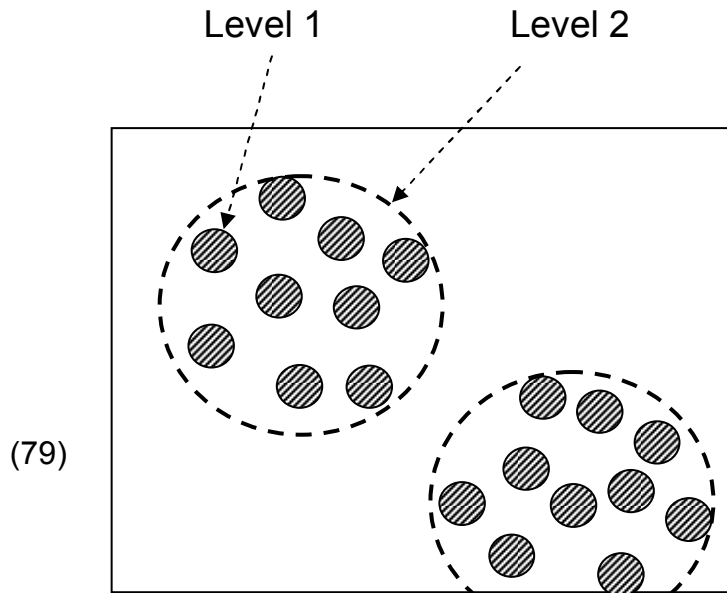
Two-level structure:

$$I(q) = \left[G_1.e^{-\frac{1}{3}R_{g1}^2 q^2} + B_1.e^{-\frac{1}{3}R_c^2 q^2} \left\{ \left[erf\left(qR_{g1}/6^{1/2} \right) \right]^3 / q \right\}^4 \right] . + . \left[G_2.e^{-\frac{1}{3}R_{g2}^2 q^2} + B_2 . \left\{ \left[erf\left(qR_{g2}/6^{1/2} \right) \right]^3 / q \right\}^4 \right]$$

$$I(q) = \sum_{i=1}^{n} \left[G_i.e^{-\frac{1}{3}R_{gi}^2 q^2} + B_1.e^{-\frac{1}{3}R_{g(i+1)}^2 q^2} \left\{ \left[erf\left(qR_{gi}/6^{1/2} \right) \right]^3 / q \right\}^4 \right]$$

Fractal objects: $I(q) = N.I_1(q).S(q)$
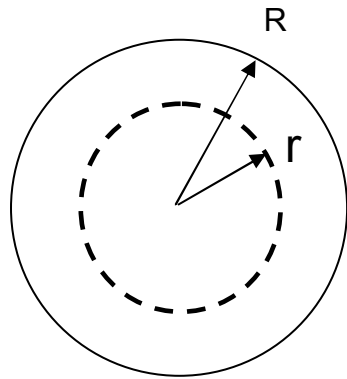
Homogeneous object

$$M(r) = a.r^3$$

Fractal object

$$M(r) = a.r^D \quad \text{or:} \quad N(r) = \left(\frac{r}{r_0}\right)^D$$

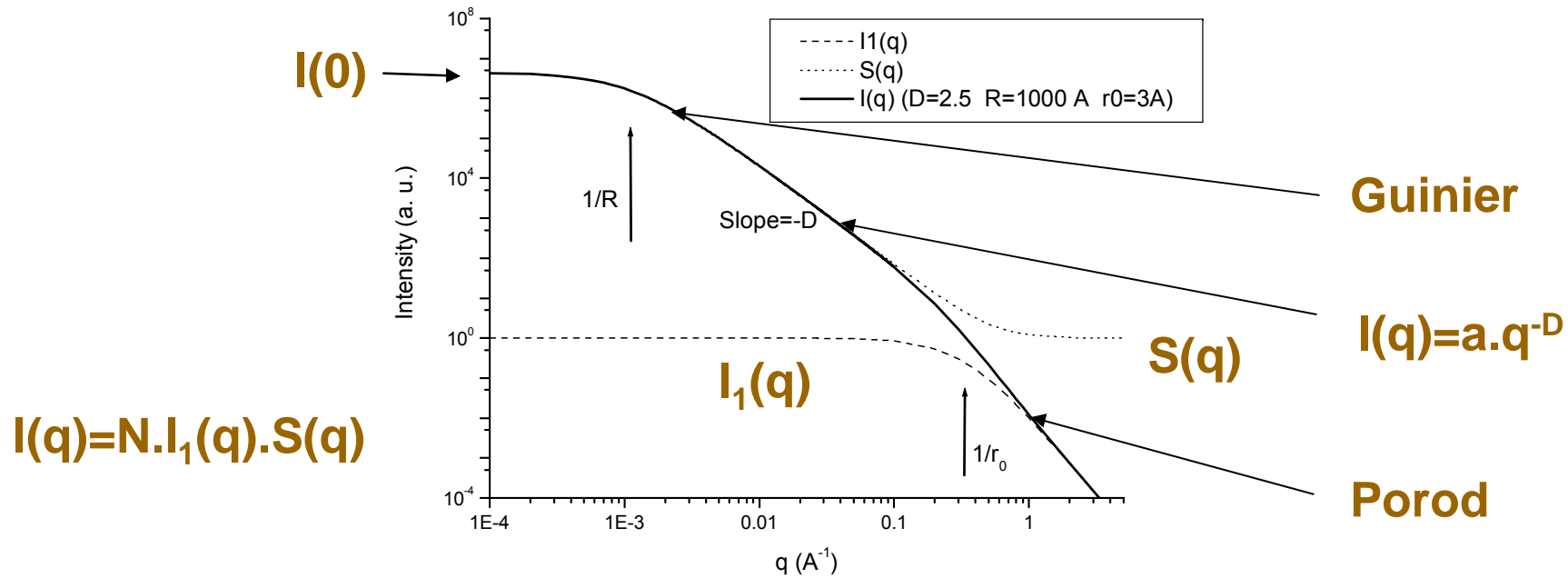$$\frac{N}{V}g(r) = \frac{N}{V} + \left(\frac{D}{4\pi r_0^D}r^{D-3}\right)e^{-r/\xi}$$

$$S(q) = 1 + \frac{D}{r_0^D}\int_0^\infty r^{D-1}e^{-\frac{r}{\xi}}\frac{\sin qr}{qr}dr$$

$$I_1(q) = \frac{A}{\left(1 + r_0^2 q^2\right)^2}$$

$$S(q) = 1 + \frac{1}{(qr_0)^D} \frac{D.\Gamma(D-1)}{\left[1 + 1/(q^2\xi^2)\right]^{(D-1)/2}} \sin\left[(D-1)\tan^{-1}(q\xi)\right]$$

$$I(q) = N.I_1(q).S(q)$$

$$I(q) = \frac{A}{\left(1 + r_0^2 q^2\right)^2} . \left\{ 1 + \frac{1}{(qr_0)^D} \frac{D.\Gamma(D-1)}{\left[1 + 1/(q^2\xi^2)\right]^{(D-1)/2}} \sin\left[(D-1)\tan^{-1}(q\xi)\right] \right\}$$

$$I(q) = N.I_1(q).S(q)$$

$$q = 0 \qquad I(0) = \Gamma(D+1).\left(\frac{\xi}{r_0}\right)^D \qquad \xi = \left[\frac{D(D+1)}{2}\right]^{-1/2} R_g \qquad I(0) = a.R_G^D$$

$$q \rightarrow 0 \quad \textbf{(Guinier)} \quad S(q) = S(0)\left\{1 - \left[\frac{D(D+1)}{6}\right]\xi^2 q^2\right\} \cong S(0).e^{-\frac{R_g^2 q^2}{3}} \qquad R_g = \left[\frac{D(D+1)}{2}\right]^{1/2} \xi$$

$$1/\xi << q << 1/r_0 \qquad I(q) \propto q^{-D}$$

$$q >> 1/ro \qquad \textbf{(Porod)} \qquad I(q) \propto q^{-4}$$

$$I(q) = N.I_1(q).S(q)$$
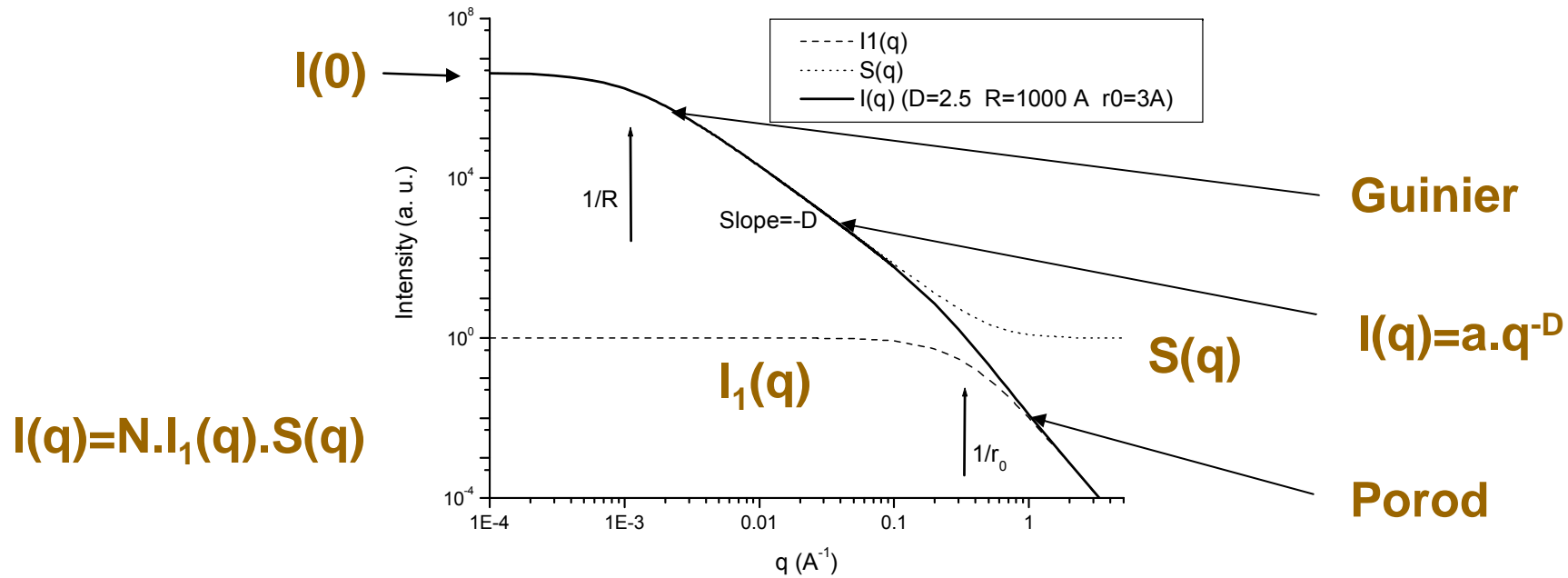
$$q = 0 \qquad I(0) = \Gamma(D+1).\left(\frac{\xi}{r_0}\right)^D \qquad \xi = \left[\frac{D(D+1)}{2}\right]^{-1/2} R_g \qquad I(0) = a.R_G^D$$

$$q \to 0 \quad \textbf{(Guinier)} \quad S(q) = S(0)\left\{1 - \left[\frac{D(D+1)}{6}\right]\xi^2 q^2\right\} \cong S(0).e^{-\frac{R_g^2 q^2}{3}} \qquad R_g = \left[\frac{D(D+1)}{2}\right]^{1/2} \xi$$

$$1/\xi \ll q \ll 1/r_0 \qquad I(q) \propto q^{-D}$$

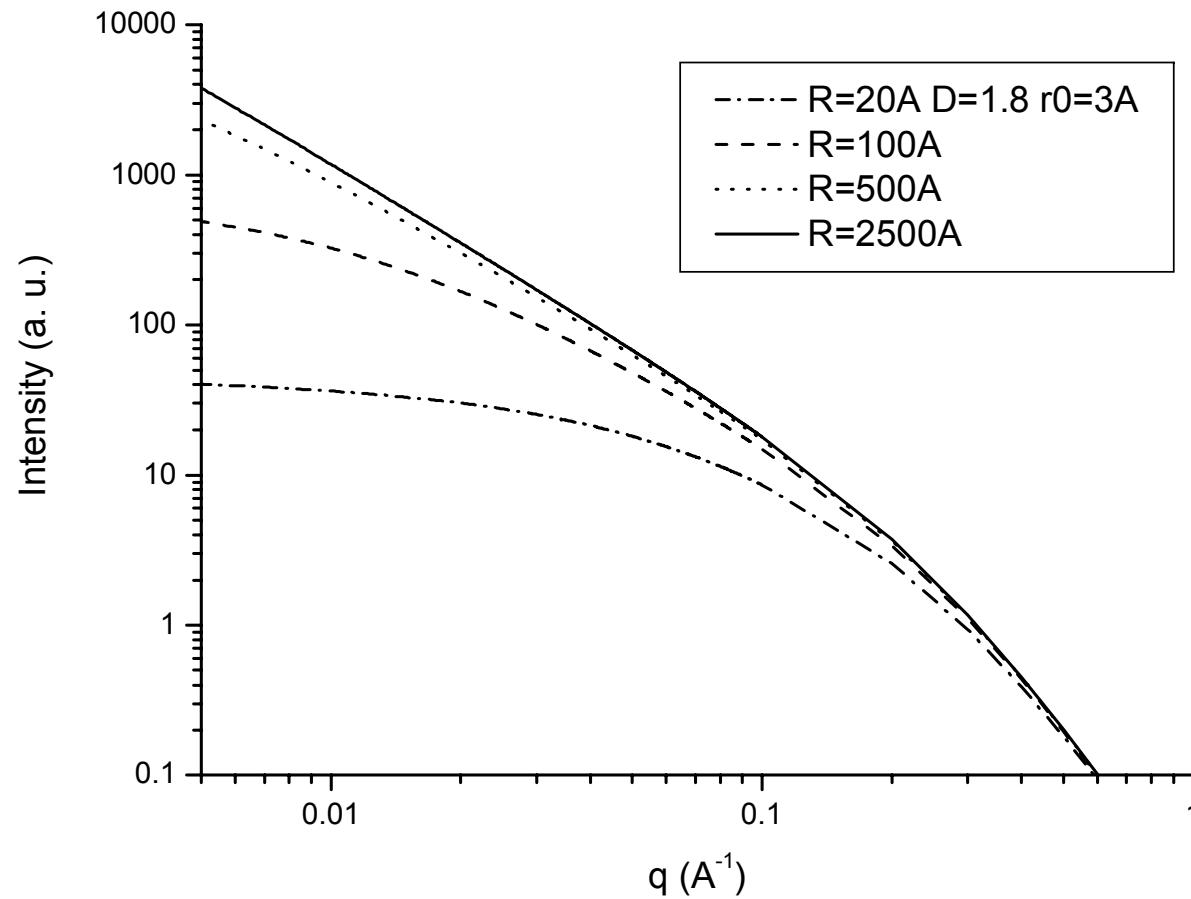$$q \gg 1/ro \qquad \textbf{(Porod)} \qquad I(q) \propto q^{-4}$$

Simulation of SAXS intensity functions for a growing cluster building up a fractal aggregate, for increasing time periods (The rather high value of the minimum q does not allow to observe the crossover 1, at low q)
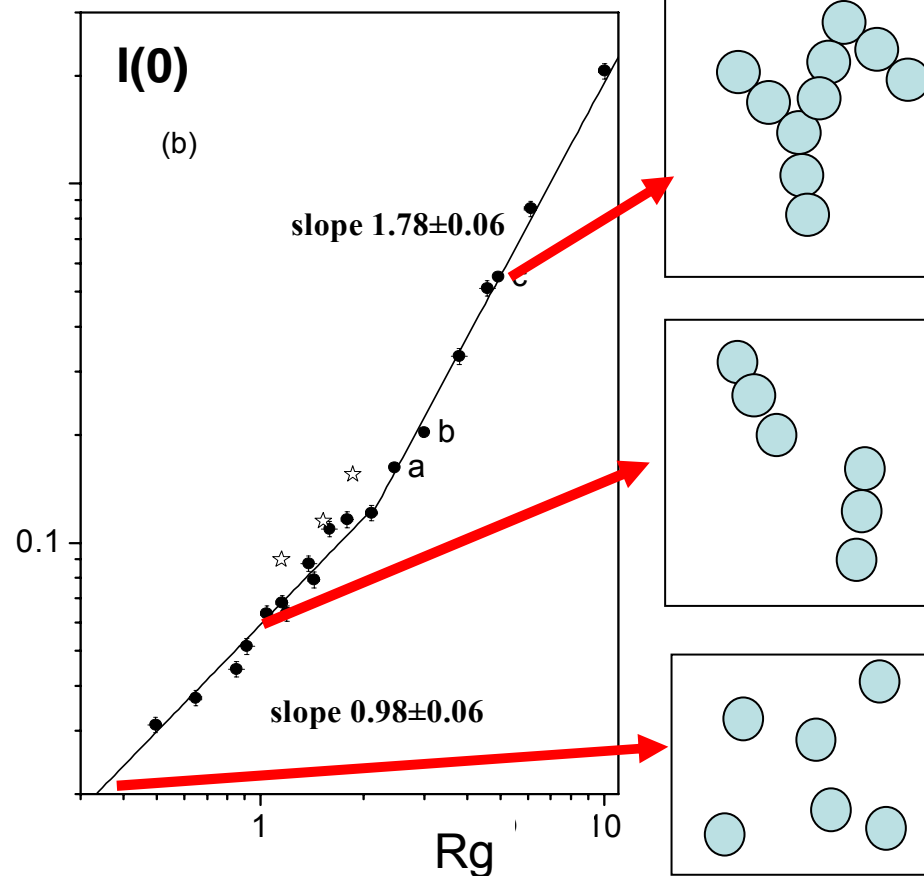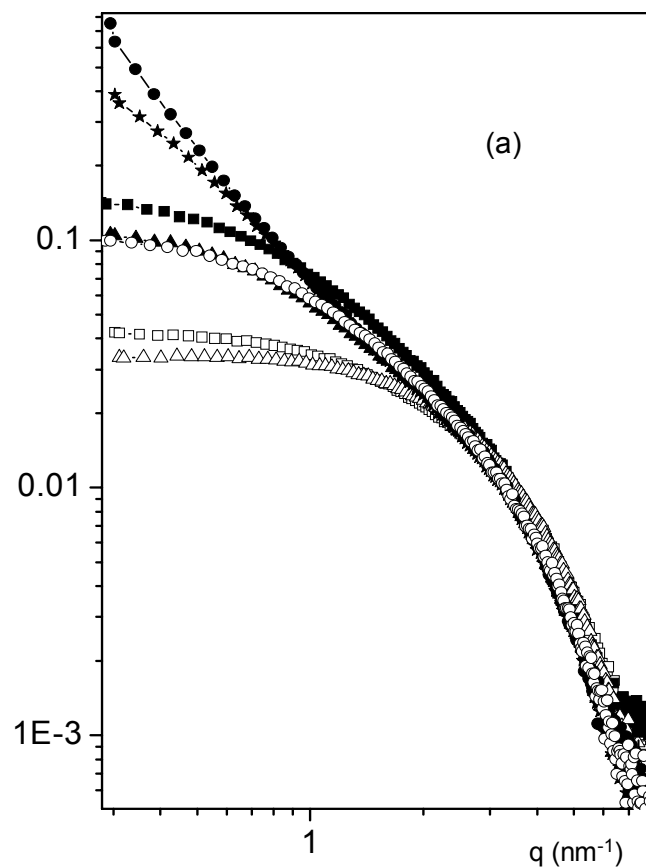
Aggregation of colloidal particles
Models of growth and results of calculations
of the fractal dimension
using computer simulation

Mechanism of growth	Fractal dimension (3D)	Fractal dimension (2D)
Eden		2
Witten Sanders	2.45	1.65-1.70
Witten Sanders linear trajectory	2.97	1.92-1.95
Tip-to-tip	1.43	1.26
Self-avoiding walk	1.66	1.33
Cluster-cluster random walk	1.75-1.80	1.44-1.48
Cluster-cluster ballistic	1.81-1.95	1.50-1.54
Ideal linear polymer	2.00	
Swollen linear polymer	1.66	
Ideal branched polymer	2.16	
Dense particle	3.00	
Diffusion limited cluster-cluster aggregation (DLCA)	1.78	
Reaction limited cluster-cluster aggregation (RLCA)	2.11	

Sulfate-zirconia sols with different HNO3, H2SO4 and H2O contents. (Riello et al)

$$I(0) = \Gamma(D+1).\left(\frac{\xi}{r_0}\right)^D = a.R_G^D$$

(a)

0.1

0.01

1E-3

1

q (nm^{-1})

(b)

I(0)

slope 1.78±0.06

c

b

a

0.1

slope 0.98±0.06

1

10

Rg

(a) Scattering intensity of several sol samples inside a sealed cell in their final aggregation state.

(b) Plot of I(0) vs. R_g, in log-log scale, corresponding to the final states of sols with different H_2SO_4 contents.

Aggregation of colloidal particles
Models of growth and results of calculations
of the fractal dimension
using computer simulation

| Mechanism of growth	Fractal dimension (3D)	Fractal dimension (2D)
Eden		2
Witten Sanders	2.45	1.65-1.70
Witten Sanders linear trajectory	2.97	1.92-1.95
Tip-to-tip	1.43	1.26
Self-avoiding walk	1.66	1.33
Cluster-cluster random walk	1.75-1.80	1.44-1.48
Cluster-cluster ballistic	1.81-1.95	1.50-1.54
Ideal linear polymer	2.00	
Swollen linear polymer	1.66	
Ideal branched polymer	2.16	
Dense particle	3.00	
Diffusion limited cluster-cluster aggregation (DLCA)	1.78	
Reaction limited cluster-cluster aggregation (RLCA)	2.11	

Nanophase separation and dynamical scaling property.
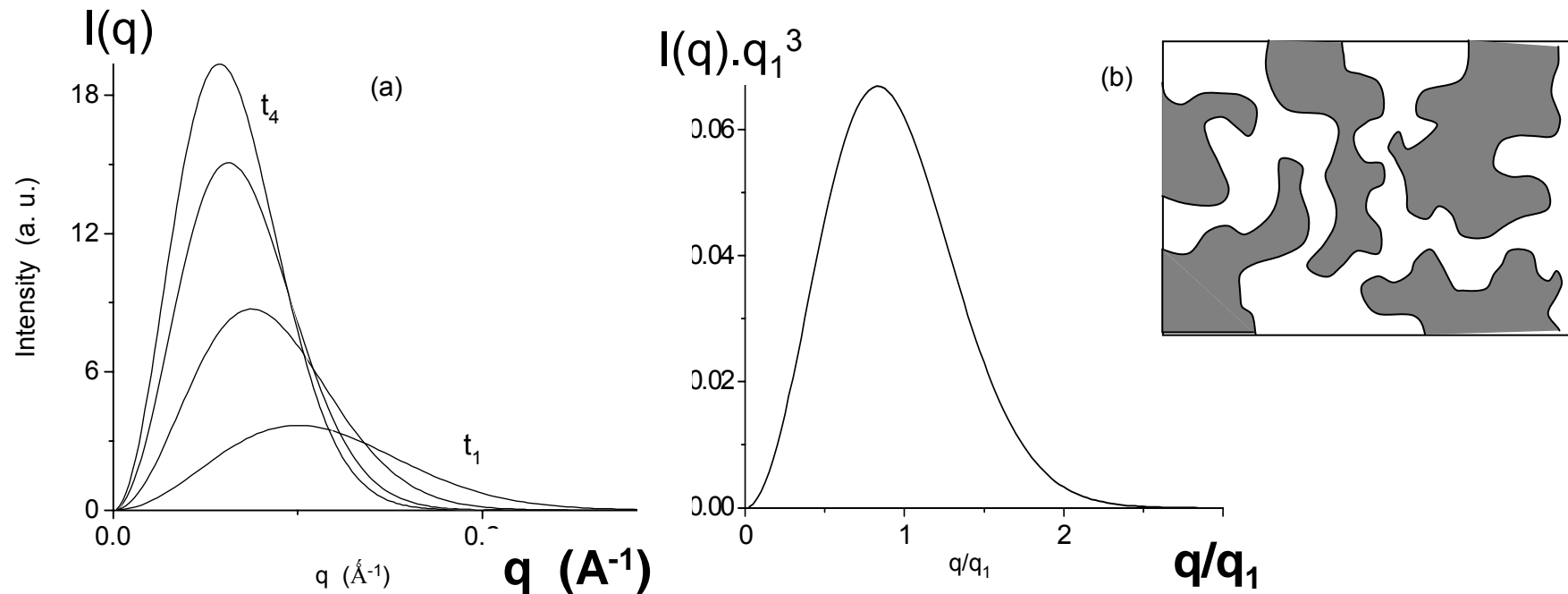
$$I(q,t) = N.I_1(q).S(q.t) \propto S(q,t)$$

$$q_n(t) = \left[\frac{\int_0^\infty q^n(t).I(q,t)dq}{\int_0^\infty I(q,t)dq} \right]^{1/n}$$

$$F(x) = I(q,t).\left[q_1(t)\right]^3$$

a) Different scattering intensity curves from a system in advanced stages of nanophase separation, for increasing periods of isothermal annealing from t_1 to t_4.
(b) Scaled structure function.

SnO2 based porous xerogels (Santilli et al)
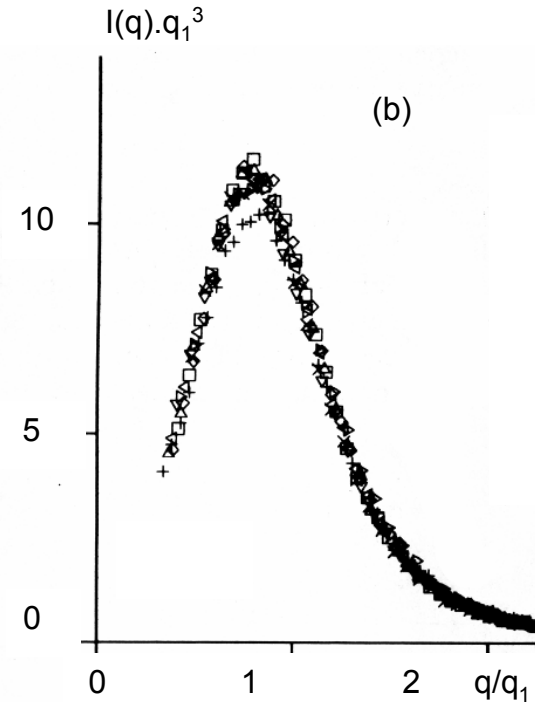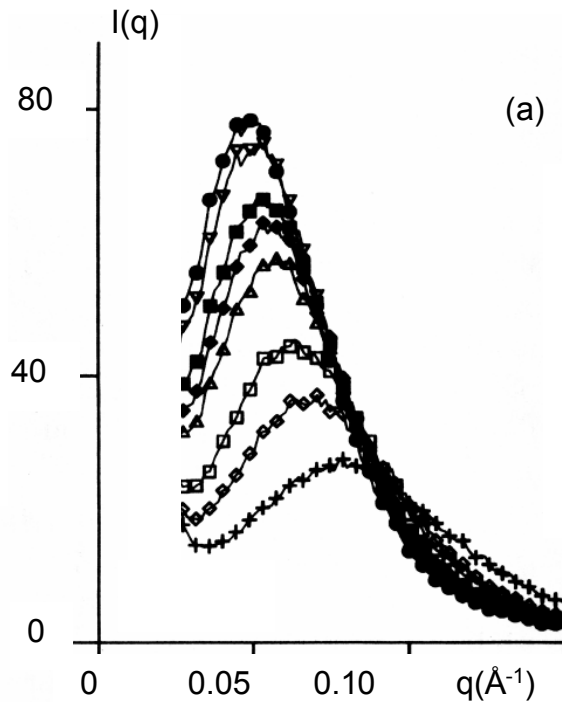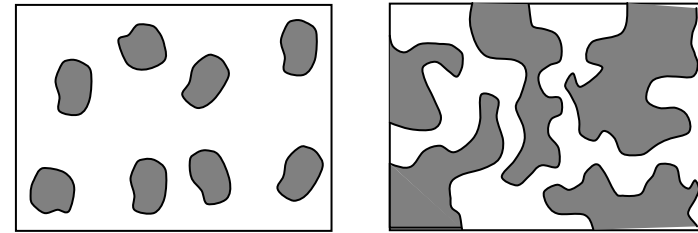
a) Scattering intensity curves corresponding to a nanoporous SnO$_2$ xerogel held at 400C during increasing periods of time from 4.5 min. (bottom) up to 62.5 min (top).
(b) Same curves plotted as [I(q,t)q$_1^3$] versus (q/q$_1$).

Zirconia-based sols (Lecomte et al)
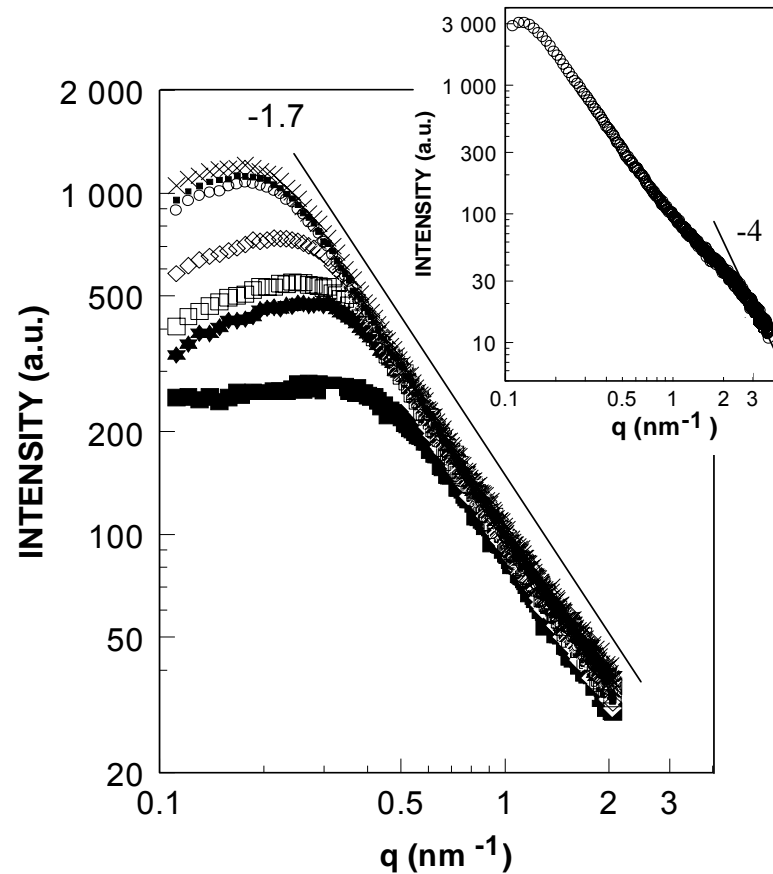
Log I vs. log q plots for increasing periods
of time from 4 hours (bottom) up to 742 hours (top).
The inset is the scattering intensity curve of the final gel

Zirconia-based sols (Lecomte et al)
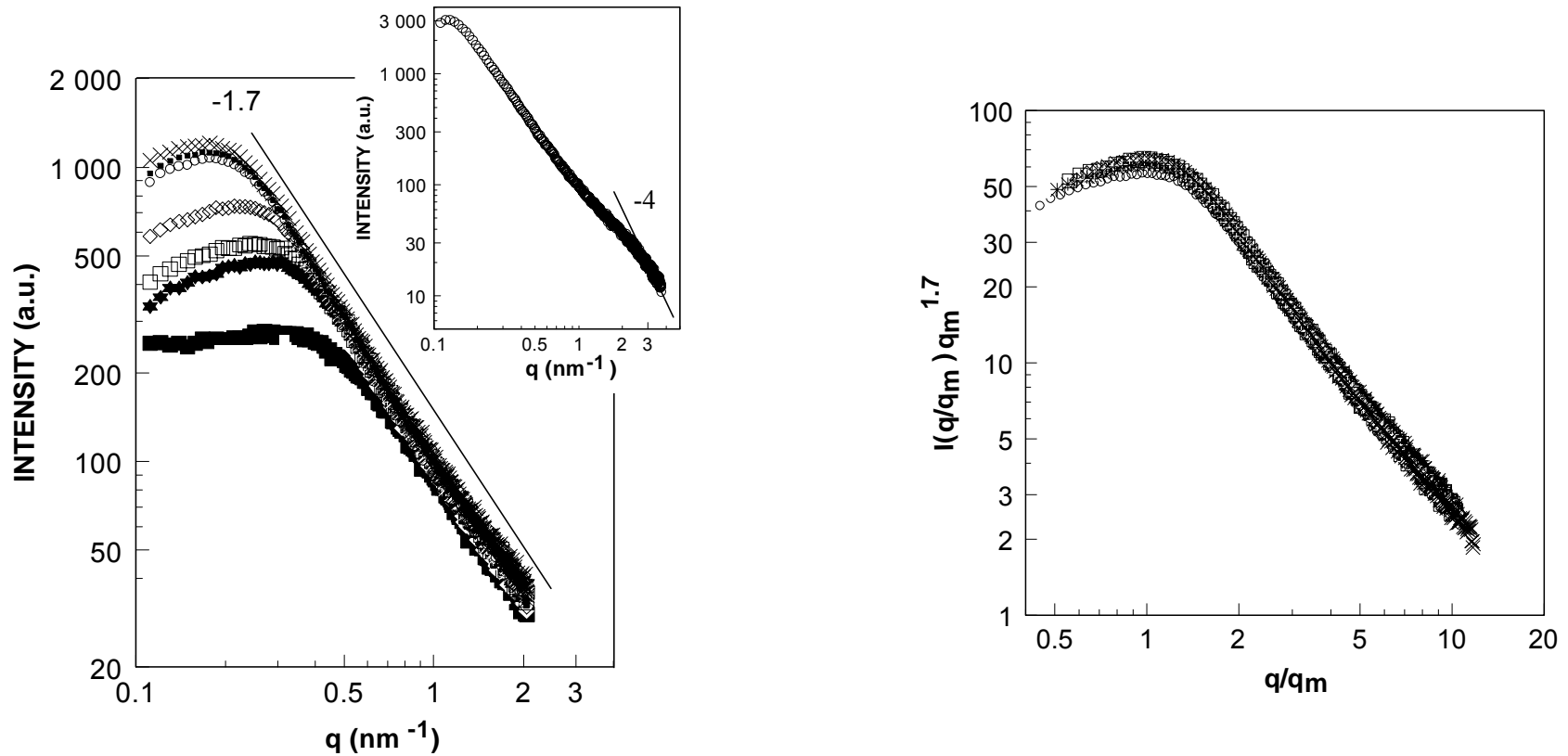
Scattering intensity curves replotted as $[I(q)q_m^{1.7}]$ versus (q/q_m), q_m being the q value corresponding to the maximum of the scattering curves (Assumption: $q_m \sim q_1$).

Anisotropic nano-objects
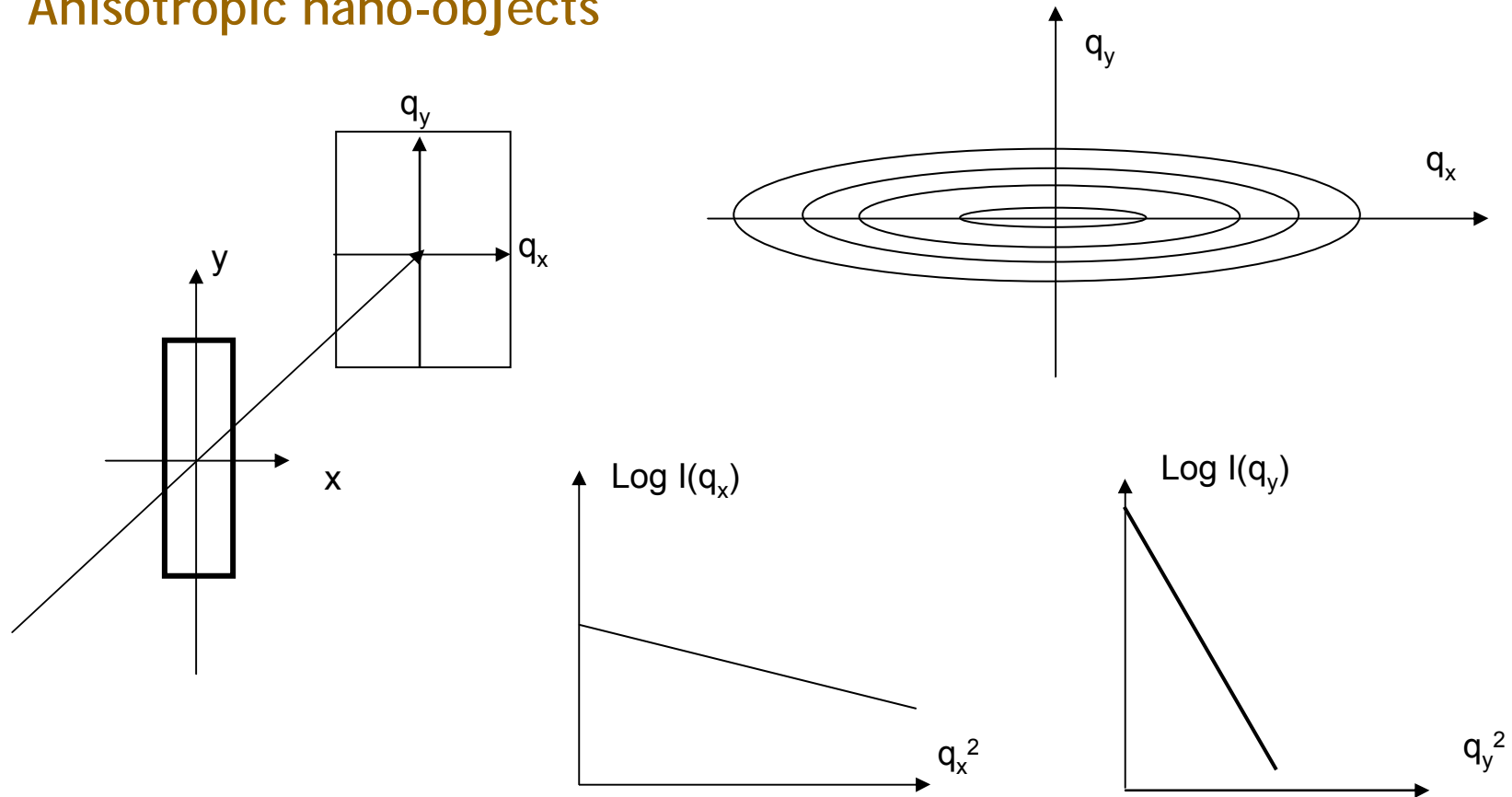
$$I_1(q_D) = N(\rho_1 - \rho_2)^2 V_1^2 e^{-R_D^2 \cdot q_D^2}$$

$$R_D = \frac{1}{V}\int_V r_D^2 . d\vec{r} = \overline{r_D^2}$$

Dilute and isotropic system of very anisotropic nano-objects

Thin needles: $\quad qI(q) \propto e^{-\frac{1}{2}R_c^2 q^2}$

Thin disks: $\quad q^2 I(q) \propto e^{-R_t^2 q^2}$
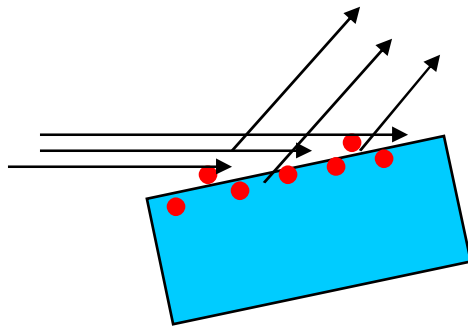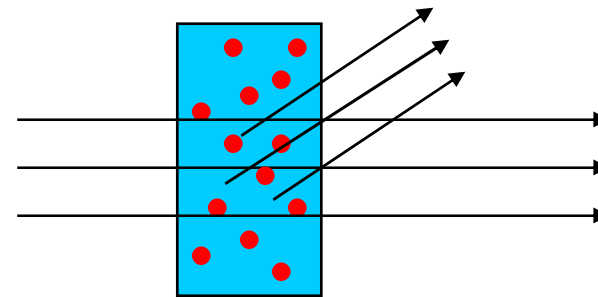
Grazing Incidence SAXS

GISAXS

GISAXS

SAXS (transmission)

both allow us to study very small objects (nanometer scale range)

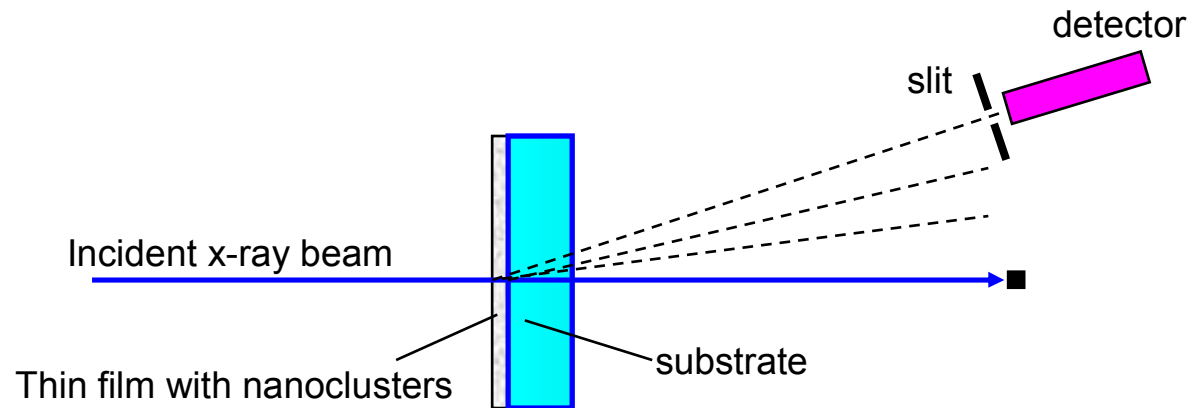small information depth is required (5 to few hundred of nanometers from top surface)

incidence and/or exit angles of the radiation must be comparable to the critical angle α_c

information is obtained over the entire irradiated volume sample

incidence normal to the sample surface

Why GISAXS?

Limitations:

- *low signal-to-background ratio*
- *low signal from thin layer film (SAXS Intensity $\propto$ irradiated volume of the sample)*
- *substrate absorption*
- *modification of the thin layer consequence of substrate thinning processes*
- *sometimes thinning is not possible*
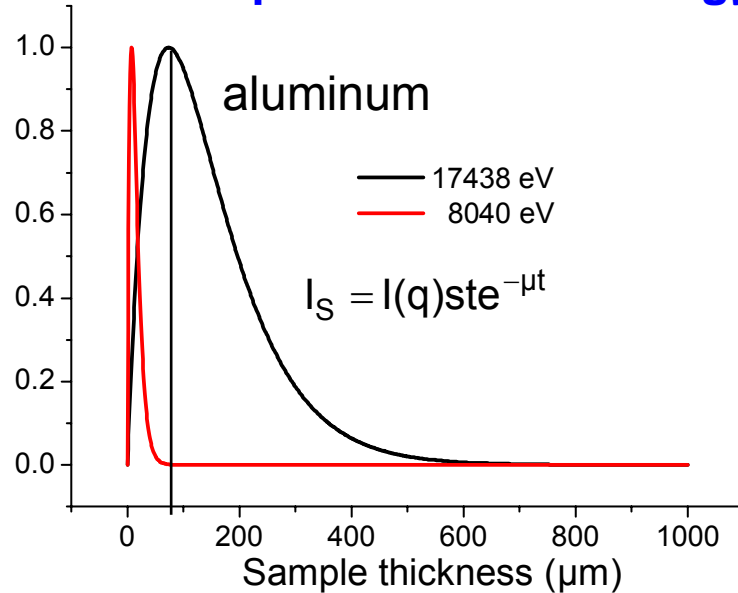
Optimization of the scattering intensity

$$I_{mesured} = I(q)ste^{-\mu(E,z_i)t}$$ scattered intensity: dependence with sample thickness

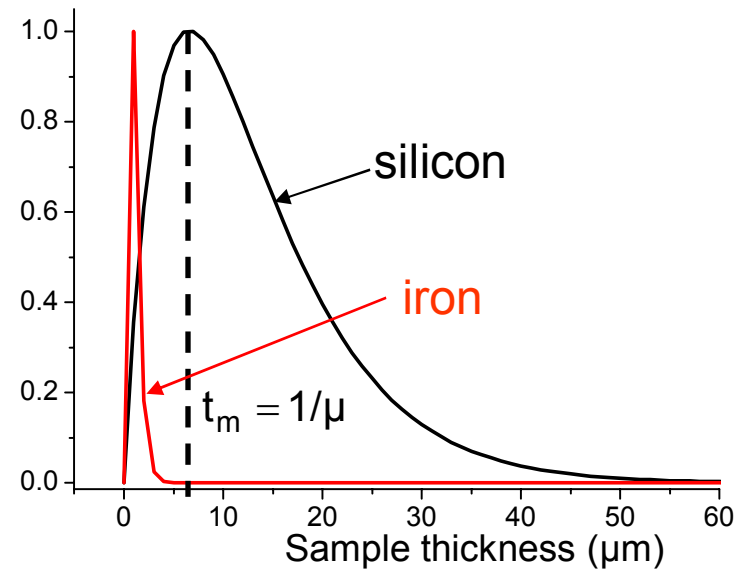s t: Irradiated volume $\begin{cases} \text{s: beam cross section area} \\ \text{t: sample thickness} \end{cases}$

$$I_0/I_t = e^{-\mu(E,z_i)t}$$ sample attenuation $\begin{cases} \mu\text{: lineal absorption coefficient} \\ E\text{: photon energy} \\ z_i\text{: atomic number of element i} \end{cases}$
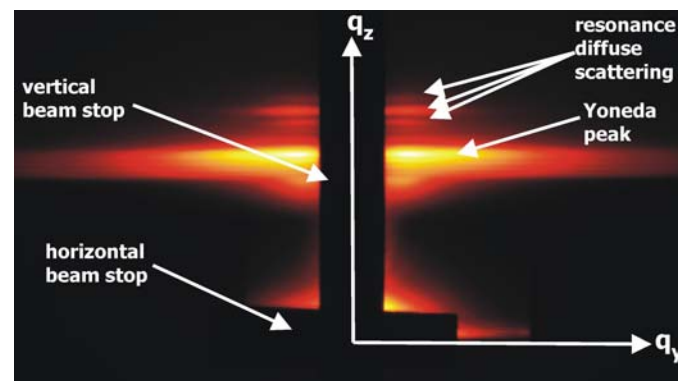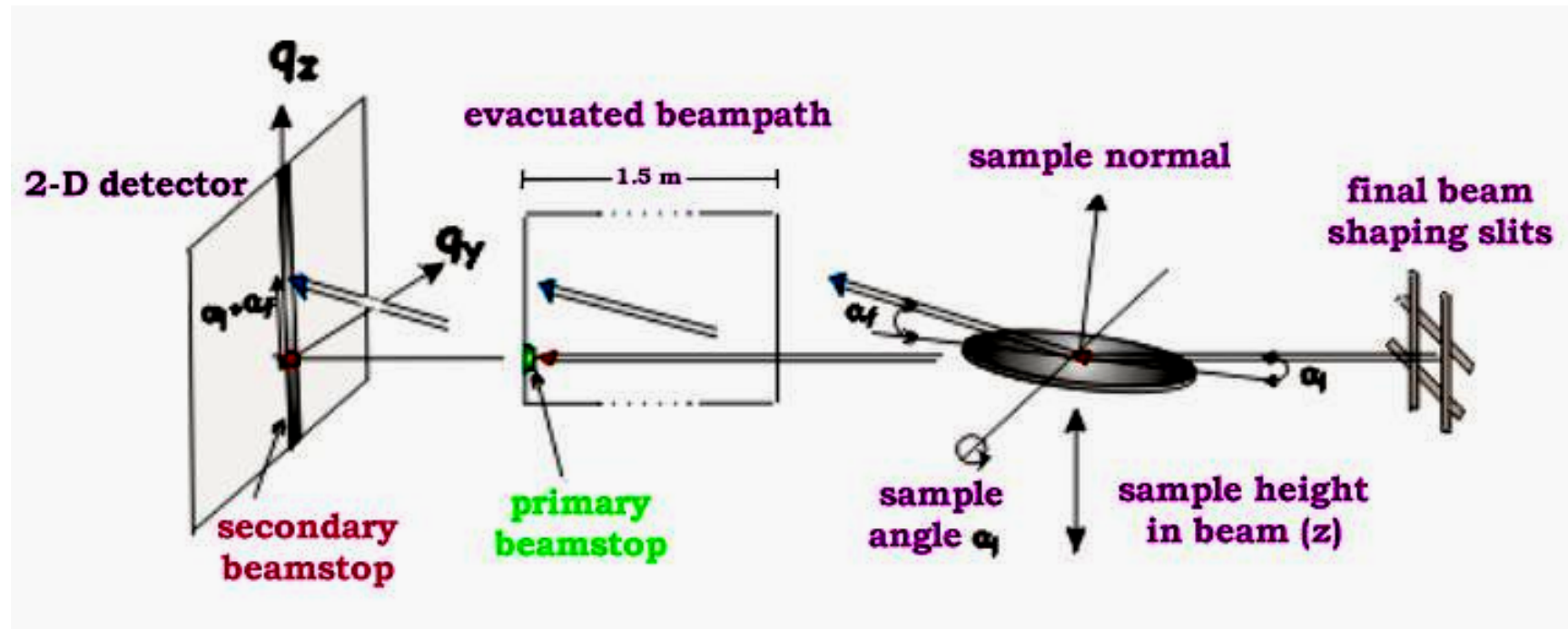
$$I_{measured} = I(q)ste^{-\mu t}$$

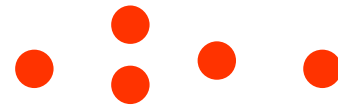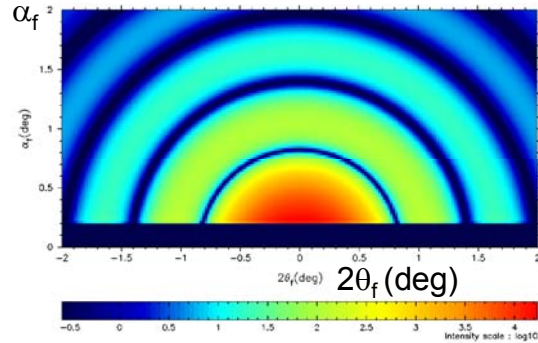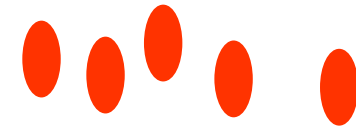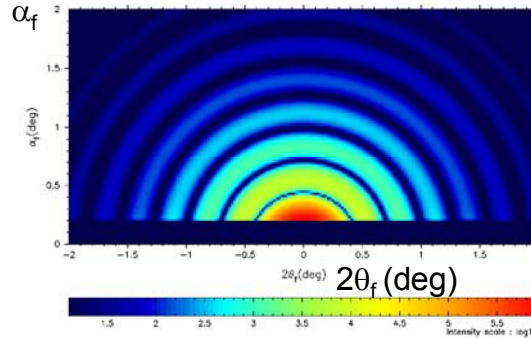**Dependence with energy**

Dependence with element

Typical experimental setup

GISAXS intensity from different objects

spheres R= 5 nm

spheres R= 10 nm

Prolate spheroid H/W=2
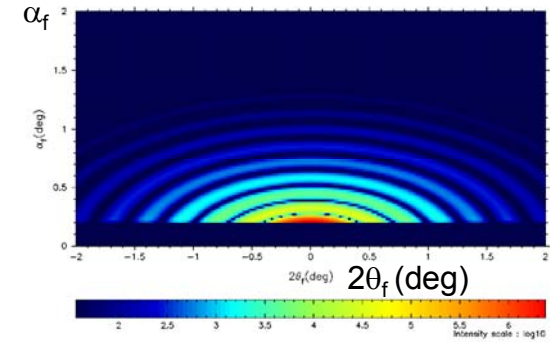
spheres ⟨R⟩= 5 nm
σ/ ⟨R⟩=0.2
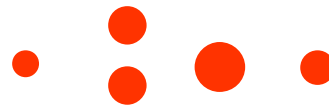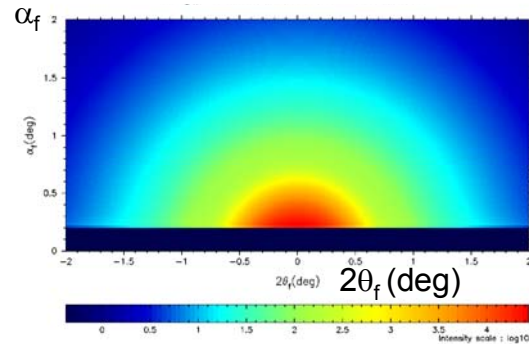
spheres ⟨R⟩= 10 nm
σ/ ⟨R⟩=0.2
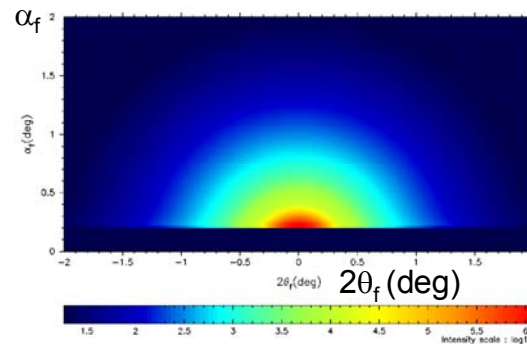
⟨R⟩= ⟨W⟩/2=10 nm
σ/ ⟨R⟩=0.2- H/W =2
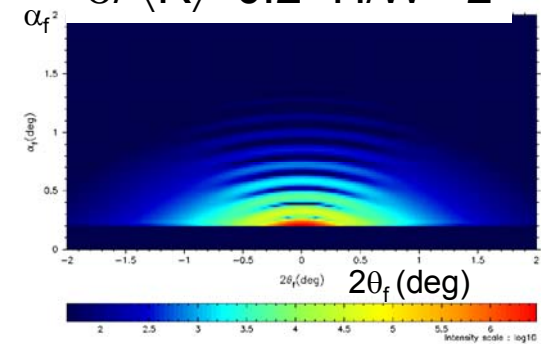
The analysis of GISAXS intensity allows determination of:

- shape
- size dispersion
- spatial ordering
- nanoparticle concentration

Examples of application:

- Studies of nanocomposite thin films

- Studies of microdomain formation and ordering in thin films and surfaces of copolymer materials

- Studies of semiconductor and metallic nanostructures (quantum dots, wires, and wells). Nanometer-sized metallic particles embedded in glass matrix (candidates for applications in the fields of nonlinear integrated optics and photonics)

Zn-based thin films prepared by sol dip coating (Tokumoto et al).
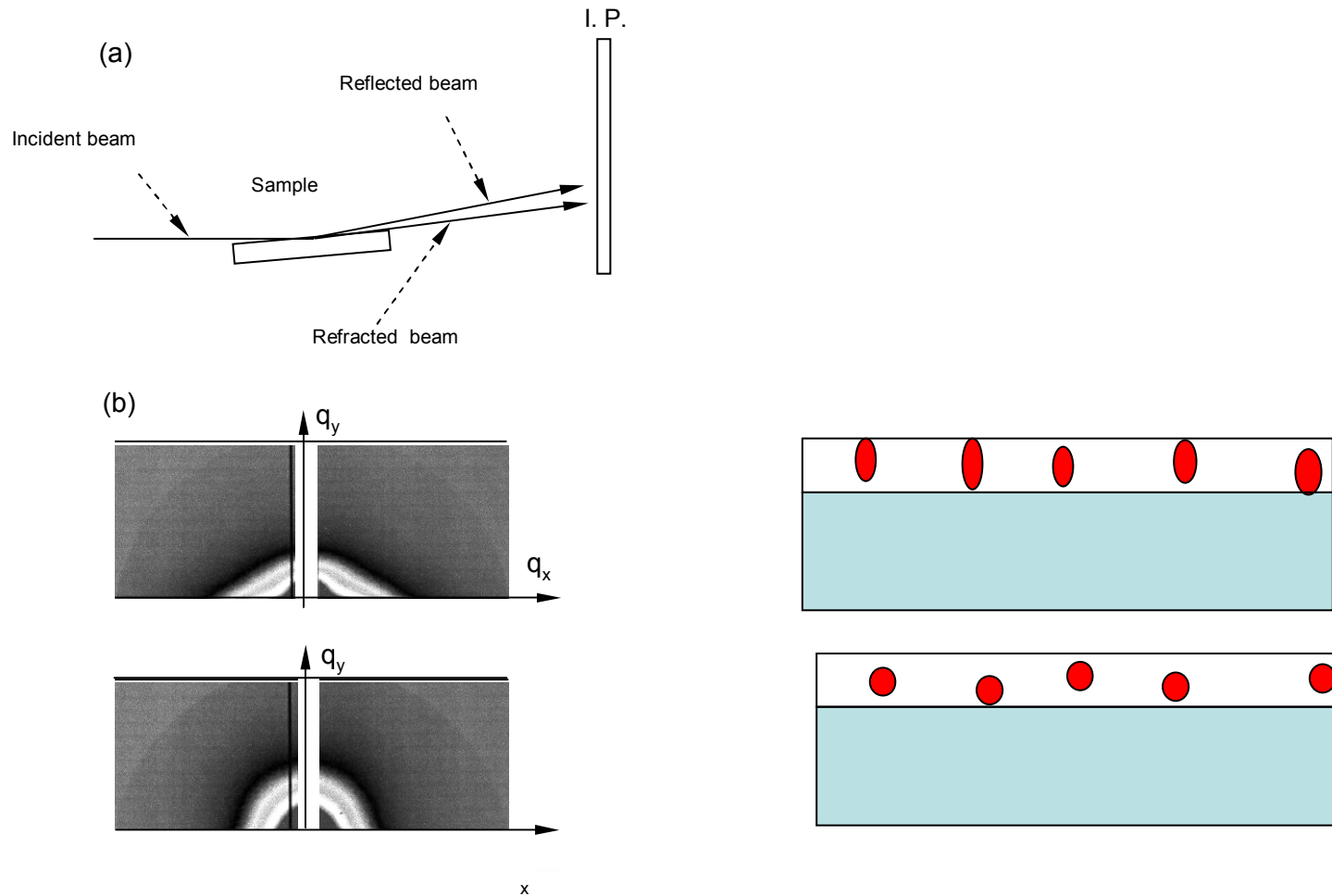
(a) Schematic GISAXS setup.
(b) GISAXS patterns recorded with an image plate
 for In-doped ZnO-based films prepared by the pyrosol procedure.
Top: Film deposited on a glass substrate at 350C.
Bottom: Film deposited on a glass substrate at 450C.

Anomalous or Resonant SAXS

ASAXS

General expression for the atomic scattering factor

The atomic scattering factor shows a sharp fluctuation in the vicinity of absorption edges

Two correction terms, f´ and f´´, must be added to account for this "anomalous" behavior

$$f_{atm}(\vec{q},E) = f_0(\vec{q}) + f'(\vec{q},E) + i\ f''(\vec{q},E)$$

(complex number)
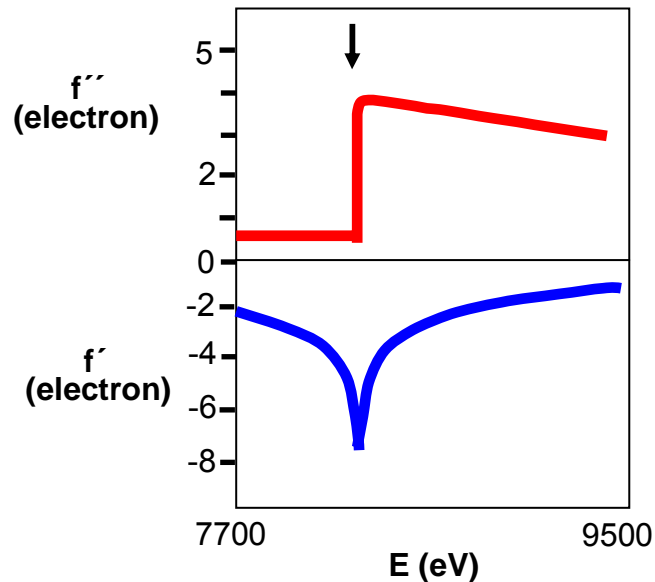
f´ and f´´ at Ni absorption edge (Z=28)
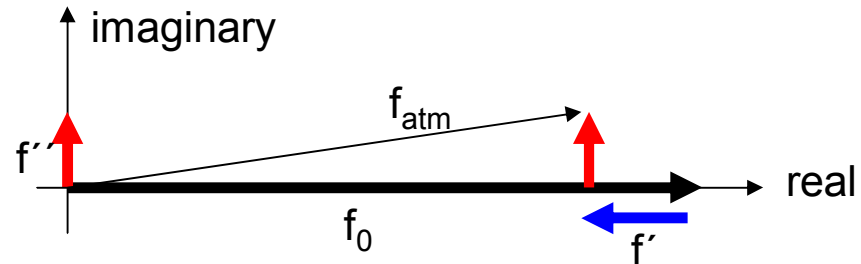
f_0 is the scattering factor far from the edge (= Z, atomic number)

f´(q,E) and f´´(q,E) are the real and imaginary part of dispersion correction. They are associated with scattering via absorption and reemission of photons, resulting in a phase shift

f´´(q,E) is weak and nearly constant below the absorption edge. It becomes more important above the edge where a strong background of fluorescence takes place

Ar / **Kr** plots of f′ and f″ versus Photon energy [eV], showing K edge and L edge features.
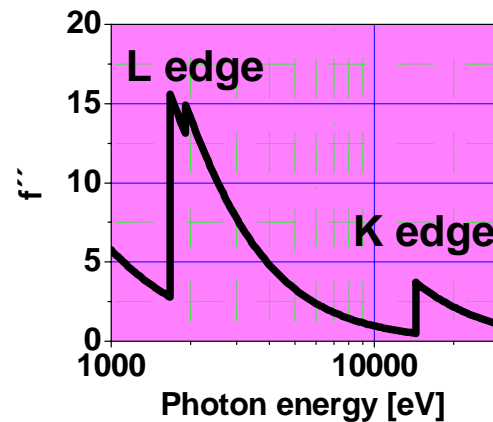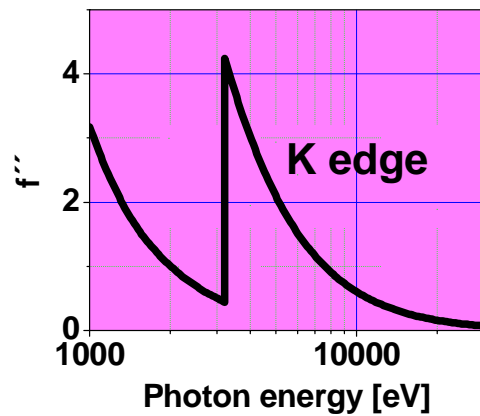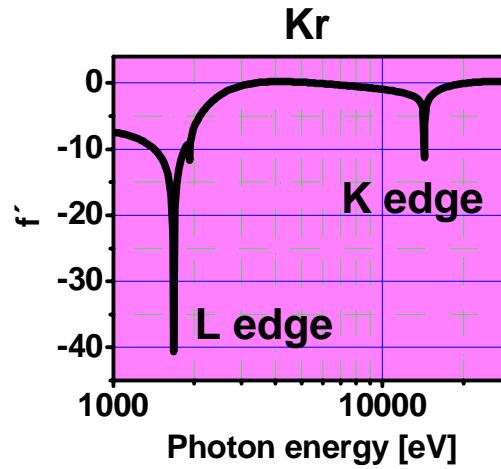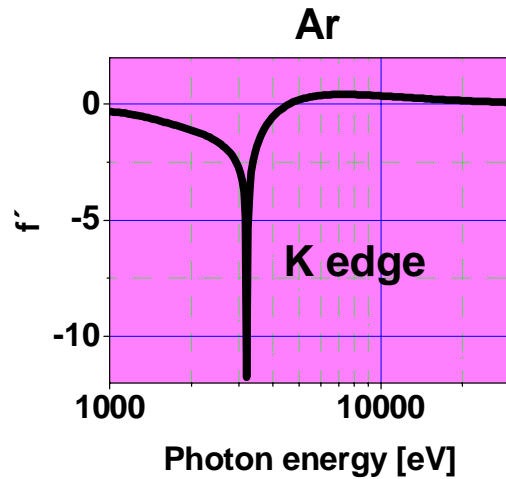
1- For heavy elements L edges falls into x-rays region.

2 - Since L shell has six $2p$ electrons compared to two electrons in the K shell, the dispersion correction in L edges are larger by a factor approximately 3.

3 - K electrons are localized close to the nucleus, so the Fourier Transform of their wavefunction is essentially constant.

So in general, the q dependence of scattering correction factors can be neglected

$$f_{atm}(\vec{q},E) = f_0(\vec{q}) + f'(E) + i\ f''(E)$$

Dependence of atomic scattering amplitude in small-angle range:

The atomic scattering intensity varies slowly with $q = 4\pi \sin\theta/\lambda$ in small-angle range

Scattered intensity (arb. units)

zoom

$$\frac{d\Sigma}{d\Omega}_{atom} = \left| f_{atom}(q) \right|^2$$

sphere (R=30 Å)
Pb atom

photon wavelength λ=1.54 Å

sphere (R=30 Å)
Pb atom

photon wavelength λ=1.54 Å

$$\frac{d\Sigma}{d\Omega}^{sphere} = \left| f_{atom}(q) * \frac{\sin(qR) - qR\cos(qR)}{(qR)^3} \right|^2$$

θ (degrees)

θ (degrees)
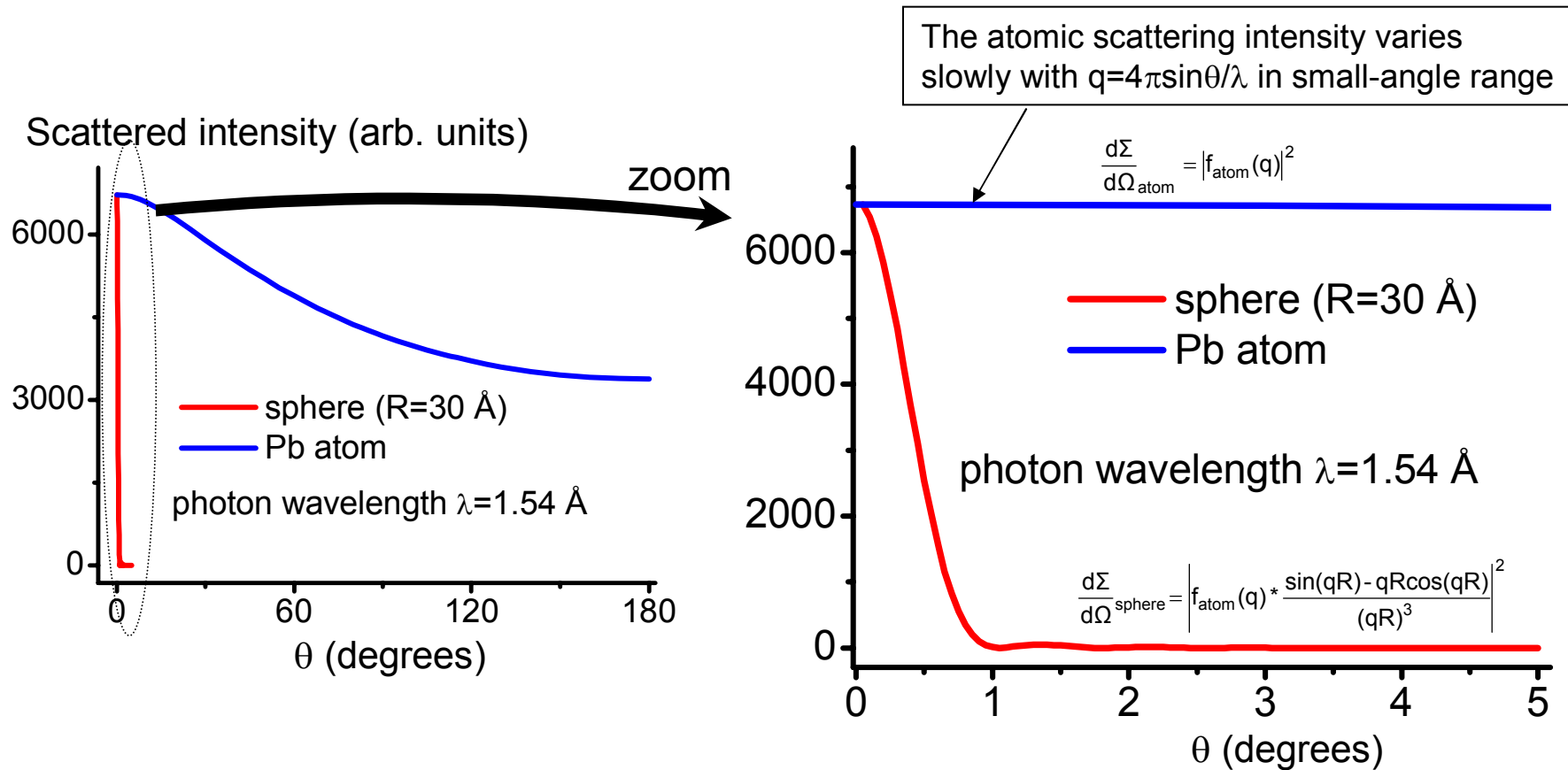
So, in small-angle region: $f_{atm}(E) = Z + f'(E) + i\ f''(E)$

Atomic form factor calculation: http://www-phys.llnl.gov/Research/scattering/fftab.html

Dependence of the atomic scattering factor with the energy for a Bi atom

For small-angles scattering: $f_{atm}(E) = Z + f'(E)$ (we assumed that $f'' << f'$)

Because f´ is a negative number, near absorption edge the atom scatters as an atom with a smaller number of electrons

$f_{Bi}(E_1 = 12981\,eV) = 83 + (-4.94) = 78.06$ electrons

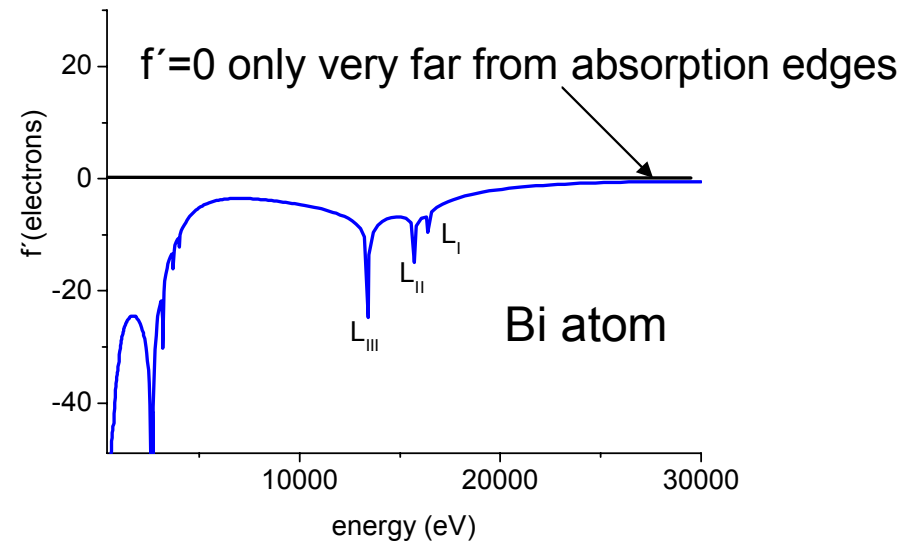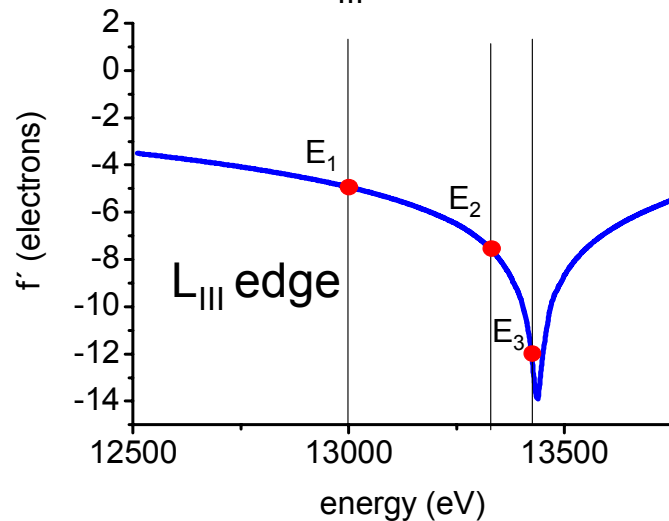$f_{Bi}(E_2 = 13319\,eV) = 83 + (-7.52) = 75.48$ electrons

$f_{Bi}(E_3 = 13413\,eV) = 83 + (-12.06) = 70.94$ electrons

Ex. Bi atom L_{III} edge: 13419 eV

SAXS intensity:
without considering the effect of anomalous scattering

$$F^i(\vec{q}) = \int [\rho(\vec{r}) - \rho_0] \exp(-i\vec{q}\cdot\vec{r}) d^3\vec{r} \quad \text{(scattering amplitude of object i)}$$

The differential scattering cross section per unity volume (intensity) is given by:

$$\frac{d\Sigma}{d\Omega}(\vec{q}) = \left| \sum_i F^i(\vec{q}) \exp(-iq\cdot R^i_{||}) \right|^2$$

(waves are summed and the total intensity is equal to summed wave times it complex conjugate)

$$\rho(\vec{r}) = \frac{\sum\limits_i n_i Z_i}{\delta V(\vec{r})} \qquad \rho_0 = \left\langle \frac{\sum\limits_i n_i Z_i}{\delta V(\vec{r})} \right\rangle$$

$\rho(\vec{r})$: local electron density at the point $\vec{r}$

ρ_0 : average electron density (token over all irradiated volume of the sample

Z_i : atomic number of element i, n_i: number of atoms in the small $\delta V(\vec{r})$ volume
$\langle...\rangle$ average over the total volume
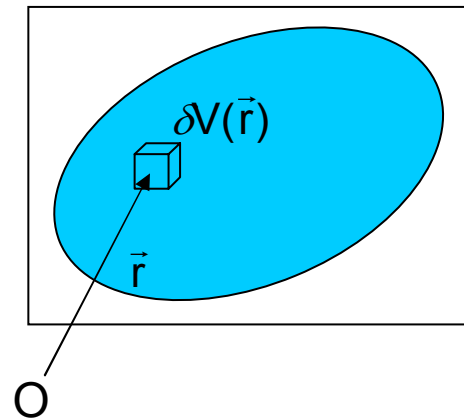
Implications of f´ in the SAXS intensity

Electron density is substituted by an "effective" electron density dependent of E:

$$\rho\ (\vec{r})\ ,\ \rho_0 \quad \rightarrow \quad \rho\ (\vec{r},E)\ ,\ \rho_0(E)$$

$$\rho\ (\vec{r},E) = \frac{\sum\limits_i n_i f_{atm}^i(E)}{\delta V(\vec{r})} \qquad \rho_0(E) = \left\langle \frac{\sum\limits_i n_i f_{atm}^i(E)}{\delta V(\vec{r})} \right\rangle \qquad f_{atm}(E) = Z + f´(E)$$

As a consequence:

$$F^i(\vec{q},E) = \int [\rho\ (\vec{r},E) - \rho_0(E)]\ \exp(-i\vec{q}\cdot\vec{r})d^3\vec{r} \quad \text{(scatt. amplitude of object i)}$$

and so, also the total SAXS intensity: $\dfrac{d\Sigma}{d\Omega}(\vec{q},E) = \left| \sum\limits_i F^i(\vec{q},E)\exp(-iq\cdot R_{||}^i) \right|^2$

depend of the photons energy

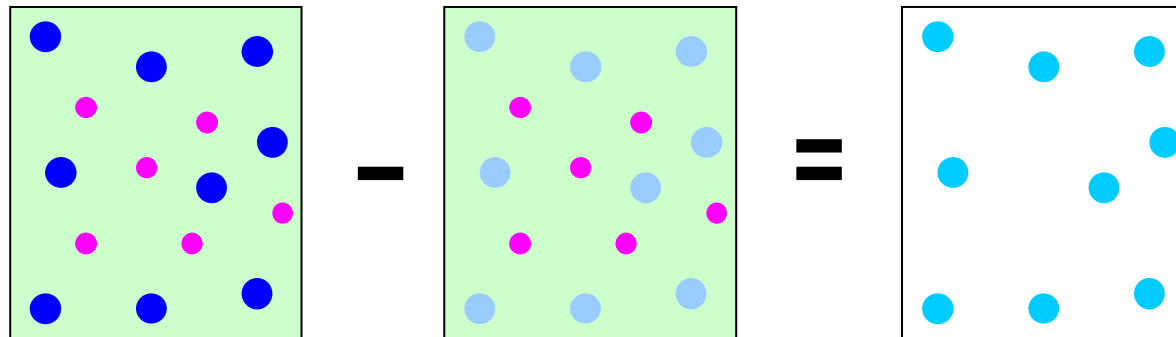The difference in the scattering intensity measured at energies E1 and E2 is given by:

$$\frac{d\Sigma}{d\Omega}(q,E_1) - \frac{d\Sigma}{d\Omega}(q,E_2) = \left[\frac{d\Sigma}{d\Omega_A}(q,E_1) + \overset{=0}{\cancel{\frac{d\Sigma}{d\Omega_B}(q)}}\right] - \left[\frac{d\Sigma}{d\Omega_A}(q,E_2) + \cancel{\frac{d\Sigma}{d\Omega_B}(q)}\right]$$

$$\frac{d\Sigma}{d\Omega}(q,E_1) - \frac{d\Sigma}{d\Omega}(q,E_2) = \frac{d\Sigma}{d\Omega_A}(q,E_1) - \frac{d\Sigma}{d\Omega_A}(q,E_2)$$

From the difference only the contribution of element A is obtained:

$$\frac{d\Sigma}{d\Omega}(q,E_1) - \frac{d\Sigma}{d\Omega}(q,E_2) = N_A |F(q,R_A)|^2 \left\{[\rho_A(E_1) - \rho_0]^2 - [\rho_A(E_2) - \rho_0]^2\right\}$$
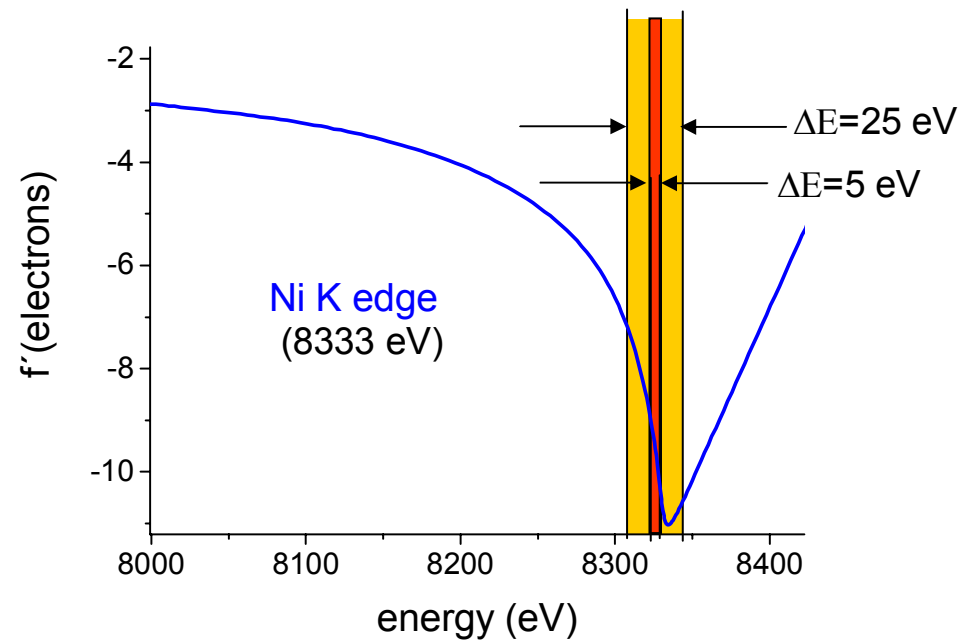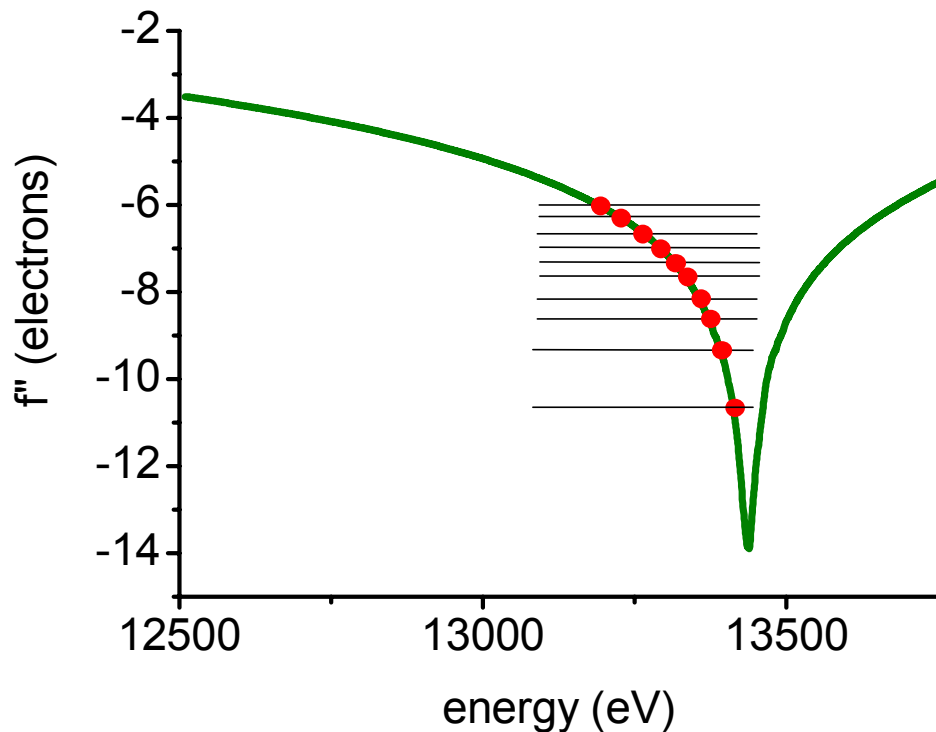
High energy resolution

Because the anomalous effects are larger in a narrow energy range near the absorption edge, a high energy resolution is a pre-requisite to any ASAXS experiment

In general $\Delta E/E \sim 10^{-4}$ or at least 10^{-3} is necessary

Choice of photons energy

- Measurements has to be performed as much as possible near the absorption edge to enhance the variation of f_{atom}

- Always below the absorption edge to avoid fluorescence (typically 5-15 eV below depending of the energy resolution)

- The number of measured energies depend of the information you are looking for

- Different elements in same sample can be probed (different edges)

- If different edges are studied sample thickness must be adjusted allowing for acceptable attenuation

ASAXS from Bi nanocrystals embedded in sodium borate glass
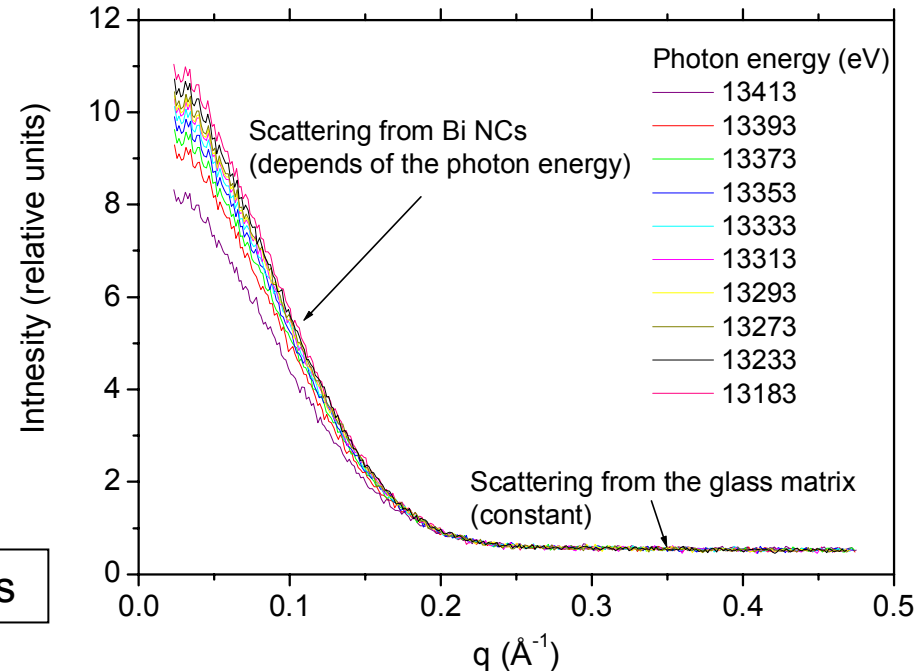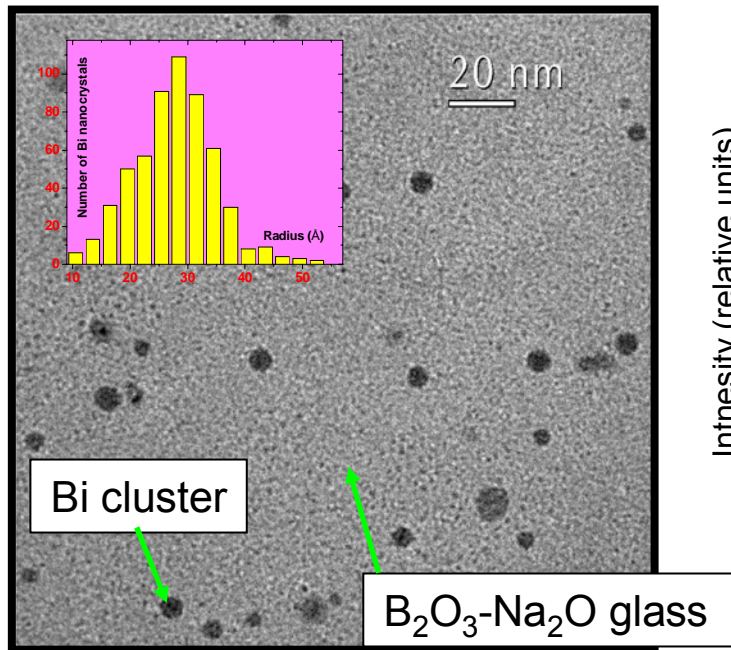
SAXS intensity as a function of the x-ray energy measured using a position-sensitive detector. A progressive decrease in the scattering intensity is observed for a continuous increase in the photon energy from 13,183 up to 13,413 eV. This is the expected behavior due to the reduction of the atomic scattering factor when the photon energy approximates to the energy of the Bi absorption edge. On the other hand, for high q values, where the SAXS intensity of Bi clusters is small, a q and $energy$ independent intensity is still observed. This q independent intensity is known to be due to fluctuation in the glass matrix density in nanometric scale dimension. Since for the studied composite all Bi atoms are inside the Bi nanocrystals they do not contribute to the matrix scattering intensity and so also no dependence with the energy is expected for it.

Scattering cross section per sample unity volume $\dfrac{d\Sigma}{d\Omega}_{tot}(\vec{q},E) = \dfrac{d\Sigma}{d\Omega}_{cat}(\vec{q},E) + \dfrac{d\Sigma}{d\Omega}_{pore}(\vec{q})$

$\dfrac{d\Sigma}{d\Omega}_{cat}(\vec{q},E)$ scattering from Pt particles and $\dfrac{d\Sigma}{d\Omega}_{cat}(\vec{q},E)$ scattering from Pt particles

$$\frac{d\Sigma}{d\Omega}_{cat}(\vec{q}) = (n_{Pt}f_{Pt} - n_M f_M)^2 \frac{N}{V_s} \int N(R)|F(\vec{q},R)|^2 v(R)^2 dR \qquad v(R) = \frac{4}{3}\pi R^3$$

since $n_{Pt}f_{Pt} \gg n_M f_M$

$$\boxed{\frac{d\Sigma}{d\Omega}_{cat}(\vec{q}) = (n_{Pt}f_{Pt})^2 \frac{N}{V_s} \int N(R)|F(\vec{q},R)|^2 v(R)^2 dR}$$

$$\boxed{\text{sphere form factor} \qquad |F(\vec{q},R)|^2 = \left|\frac{\sin(qR) - qR\cos(qR)}{(qR)^3}\right|^2}$$

$N(R)$: radius distribution function

$\dfrac{N}{V_s}$: number of Pt nanoparticles per unity volume

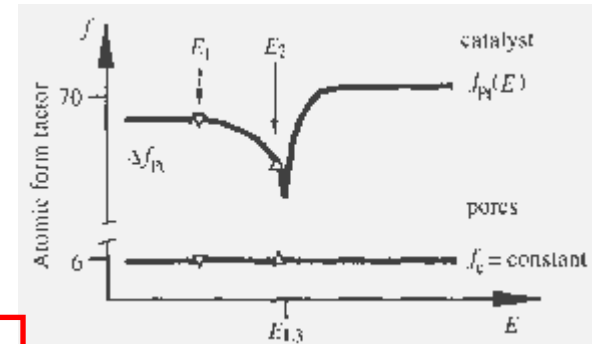$$\frac{d\Sigma}{d\Omega}_{pore}(\vec{q}) = 2\pi |n_{el}f_{el} - n_M f_M|^2 A_{pore} q^{-4}$$

From the difference of two ASAXS measurements at X-ray energies E_1 and E_2

$$\frac{d\Sigma}{d\Omega}_{tot}(\vec{q},E_1) = \frac{d\Sigma}{d\Omega}_{cat}(\vec{q},E_1) + \frac{d\Sigma}{d\Omega}_{pore}(\vec{q})$$

$$\frac{d\Sigma}{d\Omega}_{tot}(\vec{q},E_2) = \frac{d\Sigma}{d\Omega}_{cat}(\vec{q},E_2) + \frac{d\Sigma}{d\Omega}_{pore}(\vec{q})$$

$$\frac{d\Sigma}{d\Omega}_{tot}(\vec{q},E_1) - \frac{d\Sigma}{d\Omega}_{tot}(\vec{q},E_2) = \frac{d\Sigma}{d\Omega}_{cat}(\vec{q},E_1) - \frac{d\Sigma}{d\Omega}_{cat}(\vec{q},E_2)$$

Atomic scattering factors

the separated catalyst scattering is obtained:

$$\frac{N}{V_s}\int N(R)|F(\vec{q},R)|^2 v(R)^2 dR = \frac{1}{[n_{Pt}f_{Pt}(E_1)]^2 - [n_{Pt}f_{Pt}(E_2)]^2}\left[\frac{d\Sigma}{d\Omega}_{tot}(E_1) - \frac{d\Sigma}{d\Omega}_{tot}(E_2)\right]$$

Pt clusters scattering cross section
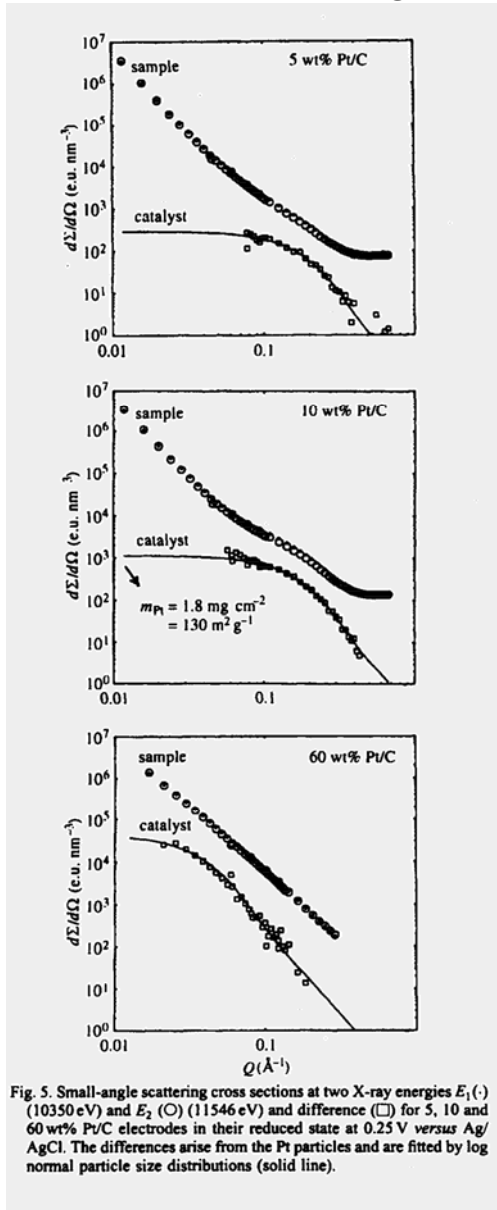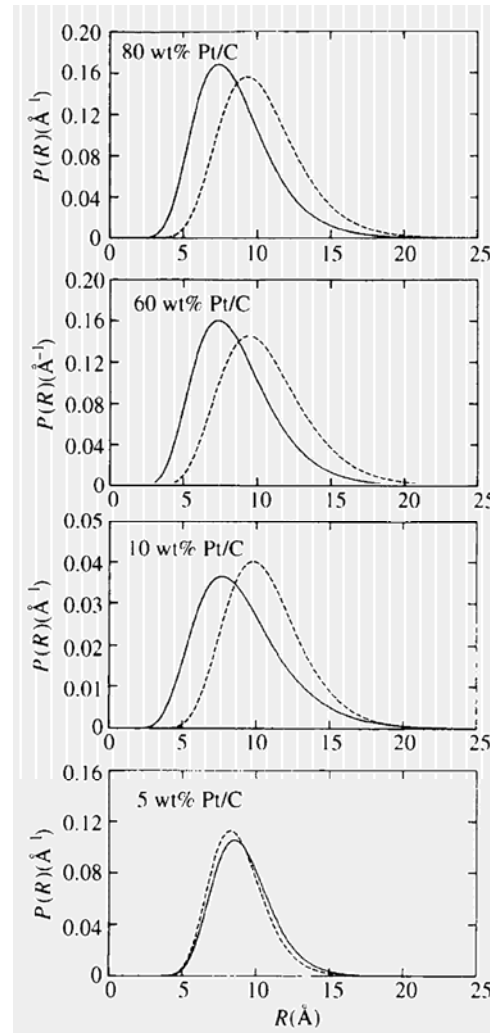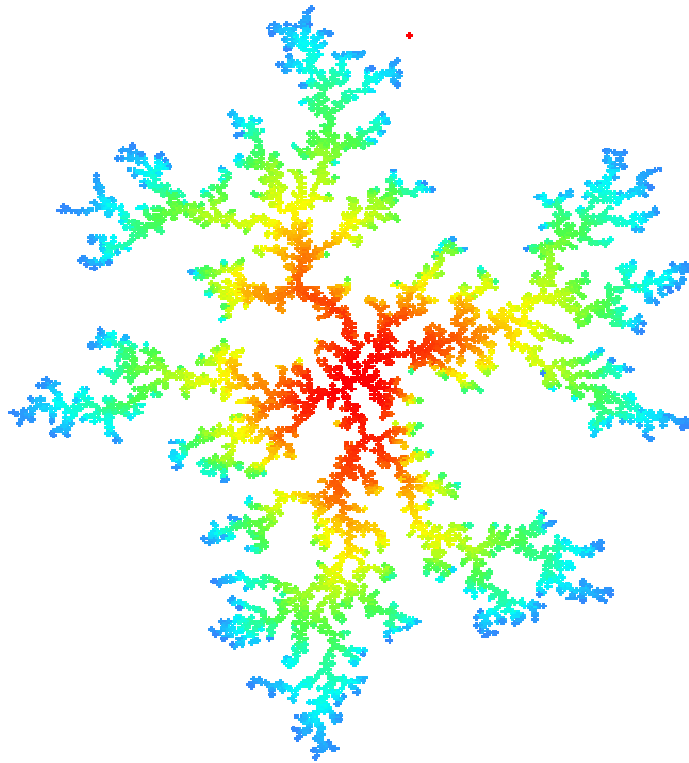
Size distribution function

Fig. 5. Small-angle scattering cross sections at two X-ray energies E_1 (·) (10350 eV) and E_2 (O) (11546 eV) and difference ($\square$) for 5, 10 and 60 wt% Pt/C electrodes in their reduced state at 0.25 V *versus* Ag/AgCl. The differences arise from the Pt particles and are fitted by log normal particle size distributions (solid line).

THE END

craievich@if.usp. br

**Cluster of colloidal particles
A fractal nano-object**

**Licurgus roman calice
Glass containing metallic nanoparticles**

Reference:
"Small-angle X-ray scattering by nanostructured materials".
A. F. Craievich.
Handbook of Sol-Gel Science and Technology.
A Sakka, Editor.
Volume II: Characterization of Sol-Gel Materials and Products.
Chapter 8, Pages 161-89 Kluwer Publishers (2005).